



Yale University
School of Medicine



Fachhochschule
Salzburg University
of Applied Sciences

***Effect of glucose concentration and insulin on human endometrial
stromal cells and their decidualization process***

BACHELORTHESIS

Student: Mag.^a Ruth Mader

Advisors: Dr. Clare Flannery, Dr. Geja Oostingh, Renate Wiltsche (MBA)

Prof. Dr. Hugh Taylor Laboratory / Department of Gynecology, Obstetrics and Reproductive Medicine,
Yale School of Medicine, New Haven, United States of America

Salzburg, 6th of June 2013

DECLARATION IN LIEU OF OATH

I hereby declare, in lieu of an oath, that the here presented bachelor thesis has been composed autonomously and without any external help. I did not use any other, than the listed references and supporting means. Furthermore, I hereby assure, that both literal and contented citations of those references have been indicated.

This thesis has not been submitted to any other examination board in inland or abroad and has not been published.

.....

Date

.....

Signature

Acknowledgement

I would like to express my gratitude and also my deepest appreciation to all who have contributed to this bachelor thesis:

In particular I want to name my supervisor Dr. Clare Flannery, who was very patient in showing me a lot of basic and needful scientific tools, Hanyia Naqvi and Olga Grechukchina who supported me in my English writing and my every-day life at the Taylor laboratory. Above all others I want to thank Gina Choe, who always helped me in every way she could and made New Haven a better place for me.

Additionally, I want to show my gratitude to Dr. Hugh Taylor, who accepted me as a student intern at Yale School of Medicine, and made it possible for me to make this great experience in the United States.

Furthermore I would also like to acknowledge my home universities contribution. My special thanks go to Dr. Geja Oosting who always supported me in coming to New Haven. Not only was she really flexible and considerate about this internship, but she was most competent in being a great supervisor of my thesis. Also, I want to say thank you to Mag. Lirk whose expertise and exceptional friendliness were most helpful and appreciated.

In addition, I want to show my great appreciations to the U.S. Marshall Plan Foundation. It was an honor for to be funded by an organization as honorable and dignified as this one is. I hope that I did contribute to the American-Austrian relationship in some little ways by coming to New Haven.

Last but not least I want to say thank you to all my family members and friends as well as to my boyfriend Dav. All of their calls, e-mails and Skype conversations offered me great emotional support and help during this time. Finally, my last thank you goes to little Susanna Lea. Yet unborn, she came all this way with me and made those three months even more special to me.

Index

1. Abstract	1
2. Introduction.....	4
2.1. Insulin	4
2.2. Decidualization of endometrial cells	7
2.2.2. Decidualization of endometrial cells	9
2.2.3. Decidualization and infertility.....	11
2.3. Correlation of insulin, decidualization and infertility.....	12
2.3.1. Effects of insulin on fertility	13
2.3.2. Effects of insulin on decidualization – study design.....	14
3. Materials and methods.....	16
3.1. Materials	16
3.2. Treatment plans	16
3.2.1. Growth Curve	16
3.2.2. Decidualization Project	18
3.3. Laboratory techniques	20
3.3.1. Cell culture	20
3.3.2. ELISA	22
3.3.3. mRNA extraction, formation of cDNA and qRT-PCR	24
4. Results.....	29
4.1. Growth curve.....	29
4.2. Decidualization project	31
4.2.1. ELISA analysis	31
5. Discussion and conclusion	35
6. References	37
7. Table of figures	39
8. Appendix	42

1. Abstract

Decidualization is a monthly occurring process of the endometrium which creates an optimal environment for the implantation of an embryo. As a consequence of hormonal stimulation, human endometrial stromal cells (HESCs) undergo functional and morphological changes. During decidualization, glycogen and lipids are stored in the luminal surface of the endometrium, which gives nutritional support to the implanted embryo. Recent studies have shown that diseases affecting the physiological metabolism of glucose may impair fertility rates and fecundability. Obese women as well as women with type 2 diabetes mellitus or polycystic ovary syndrome are more likely to experience difficulties becoming pregnant. Also, their pregnancy loss rates are above average.

The here presented bachelor thesis aimed to investigate the direct effect of glucose concentration and insulin on HESCs. Growth curves were performed to compare the growth pattern of HESCs in low glucose medium (1 g/dl glucose) and high glucose medium (4.5 g/dl glucose) +/- insulin. Moreover, an eight day protocol was performed to mimic decidualization *in vitro* by culturing HESCs in different media containing estradiol, medroxyprogesterone and different doses of glucose and insulin. Decidualization outcomes were measured by analyzing the expression levels of prolactin by qRT-PCR. In addition, pictures of cell morphology were taken.

The data of the cell counts showed that HESC numbers increased significantly in low glucose media compared to high glucose media; insulin doses however did not affect proliferation rates. The *in vitro* decidualization data suggested that cell differentiation was more successful in the presence of high glucose media and insulin. In summary, this preliminary data indicates that low glucose contributes to improved cell growth while high glucose plus insulin induces cell differentiation.

Unfortunately, the experiments were complicated by cell death during cell culture processes. Also, the housekeeping gene actin was not stably expressed across different treatment groups, which likely correlates with cell death, but alters the calculations of prolactin gene expression. Therefore, it is recommended to repeat both experiments with a constant number of healthy growing cells. If the results are reproducible, it is likely that glucose concentration and insulin play a key role in well-functioning decidualization processes and successful pregnancy outcomes.

Keywords: decidualization, insulin, glucose, growth curve

Zusammenfassung

Der Begriff Dezidualisierung beschreibt einen monatlichen Entwicklungsprozess des weiblichen Endometriums, welcher darauf abzielt, optimale Bedingungen für die Einnistung eines Embryos in die Gebärmutterschleimhaut zu schaffen. Durch Einlagerungen von Glukagon und Lipiden kommt es dabei zu einer funktionalen und morphologischen Veränderung der Stromazellen des Endometriums (HESCs). Wissenschaftliche Studien der vergangenen Jahre belegen, dass Erkrankungen, welche den physiologischen Glukose-Insulin-Kreislauf beeinträchtigen, negative Auswirkungen auf Fruchtbarkeits- und Schwangerschaftsraten besitzen. Übergewichtige Frauen, aber auch Frauen, welche an Diabetes 2 oder polyzystischem Ovarialsyndrom leiden, zeigen vermehrt Schwierigkeiten, schwanger zu werden. Gleichzeitig besteht für jene Frauen ein überdurchschnittliches Risiko, ihr Ungeborenes frühzeitig zu verlieren.

Diese Bachelorarbeit dient dazu, den Einfluss von verschiedenen Glukosekonzentrationen und Insulin auf HESCs zu untersuchen. Dazu wurden zwei Experimente durchgeführt: eine Wachstumskurve wurde erstellt um das Wachstumsverhalten der HESCs in vier verschiedenen Kulturmedien zu beobachten und zu vergleichen (geringe Glukosekonzentration (1 g/dl Glukose) +/- 100 nM Insulin vs. Hohe Glukosekonzentration (4,5 g/dl Glucose) +/- 100 nM Insulin). Außerdem wurde der Dezidualisierungsprozess mittels eines acht-Tage-Protokolls *in vitro* nachempfunden, wobei HESCs in verschiedenen Kulturmedien, die unter anderem Estradiol, Medroxyprogesteron und wiederum verschiedene Mengen von Glucose und Insulin enthielten, herangezüchtet. Das Ergebnis der Zelldifferenzierung wurde anhand der Prolaktinexpression mittels qRT-PCR erfasst. Zudem wurden fortlaufend Bilder der Zellmorphologie aufgenommen.

Die Zellzählungen für die Wachstumskurven ergaben, dass HESCs bedeutend besser wachsen, wenn sie in Kulturmedien mit wenig Glucose kultiviert werden. Es machte keinen Unterschied, ob diesen zusätzlich Insulin beigemischt wurde oder nicht. Die Ergebnisse der *in vitro* Dezidualisierung zeigten, dass hohe Glukosekonzentration verbunden mit Insulin, eine erhöhte Expression von Prolaktin nach sich zieht. Insgesamt führen die erhaltenen Daten zur Annahme, dass geringe Glukosekonzentrationen eher das Zellwachstum von HESCs fördern, wohingegen hohe Glukosekonzentrationen, verbunden mit Insulin, in einer gesteigerten Zelldifferenzierung resultieren.

Im Laufe der hier beschriebenen Experimente wurde unglücklicherweise vermehrt Zellsterben beobachtet. Zudem zeigten die qRT-PCR Ergebnisse, dass das Housekeeping Gen Aktin sehr variable Expressionsmuster ergaben. Deswegen sollten beide Experimente mit gesund wachsenden Zellen und einem anderen Housekeeping Gen wiederholt werden. Erst

dann wäre es möglich zu beweisen, dass Glukosekonzentrationen und Insulin eine Schlüsselrolle für einen gut funktionierenden Dezidualisierungsprozess einnehmen und infolgedessen auch den Verlauf von Schwangerschaften maßgeblich beeinflussen.

Schlüsselwörter: Dezidualisierung, Insulin, Glukose, Wachstumskurve

2. Introduction

The following text describes the background of diabetes. Moreover, the decidualization of endometrial cells is described. Thereafter, the relation between this disease and possible complications that can occur during pregnancy is established.

2.1. Insulin

Insulin is a peptide hormone that regulates carbohydrate and fat metabolism (Figure 1). It plays a crucial role in processing glucose and also influences important functions such as vascular compliance, cognition and reproductive matters as well. Several metabolic disorders, including Diabetes Mellitus (DM) Type 2 or metabolic syndrome in polycystic ovary syndrome (PCO) are associated with high insulin levels. Hyperinsulinemia likely plays a role in the pathology of hypertension or arteriosclerosis.

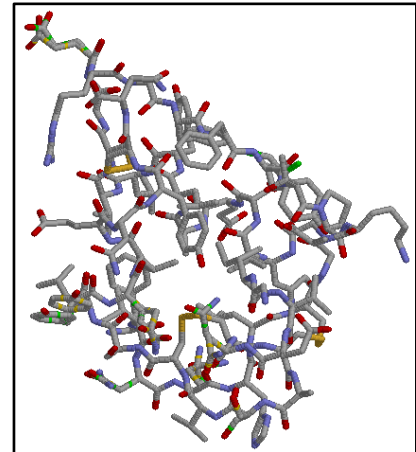


Figure 1: Insulin

Insulin is produced by β -cells of the pancreatic islets of Langerhans. These islets consist of five different cell types (α -cells, β -cells, δ -cells, PP-cells and ϵ -cells) that produce hormones such as glucagon, somatostatin and pancreatic polypeptide. β -cells constitute 65-80 % of all cells in the islets. The gene that codes for insulin is called INS and is located at the short arm of chromosome 11. It consists of about 300 nucleotides (Holt et al., 2010).

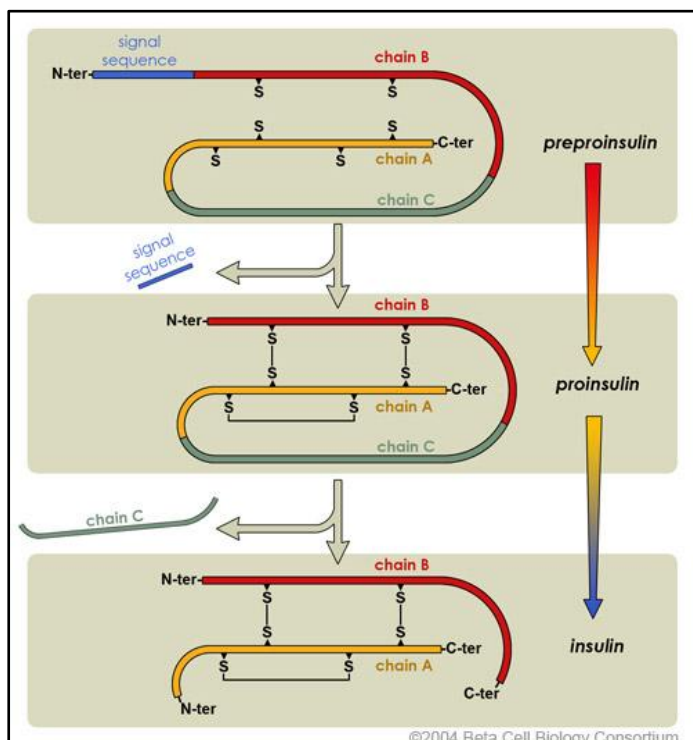


Figure 2: Insulin synthesis

In insulin synthesis, the INS gene is transcribed and translated into polypeptides by ribosomes in β -cell cytosol (Figure 2). The initial transcription product of insulin, called preproinsulin, is a 110 amino acids long single polypeptide chain. Preproinsulin includes the insulin precursor molecule proinsulin as well as a signal peptide attached to the N-terminus, which is the end of a protein or polypeptide with a free amine group. This signal peptide facilitates the translocation of the polypeptide into rough endoplasmic reticulum (RER).

Once preproinsulin reaches the lumen of the ER, the signal peptide is removed by a peptidase, thereby converting preproinsulin into proinsulin. The peptide chain then forms three disulfide bonds and folds into its tertiary structure before it is transferred to the Golgi apparatus. There, enzymes such as prohormone convertases and exoprotease carboxypeptidase E further process proinsulin into the biologically active hormone insulin. In addition, another connecting segment called the C-peptide is cleaved from the original molecule. There are two final products: insulin, which now consists of two polypeptide chains (A- and B- chain) that are linked together by disulfide bonds, and the isolated C-peptide. Both are stored in secretory vesicles in the Golgi apparatus of β -cells until metabolic signals and vagal nerve stimulation induces their release into the circulation (Jameson et al., 2010).

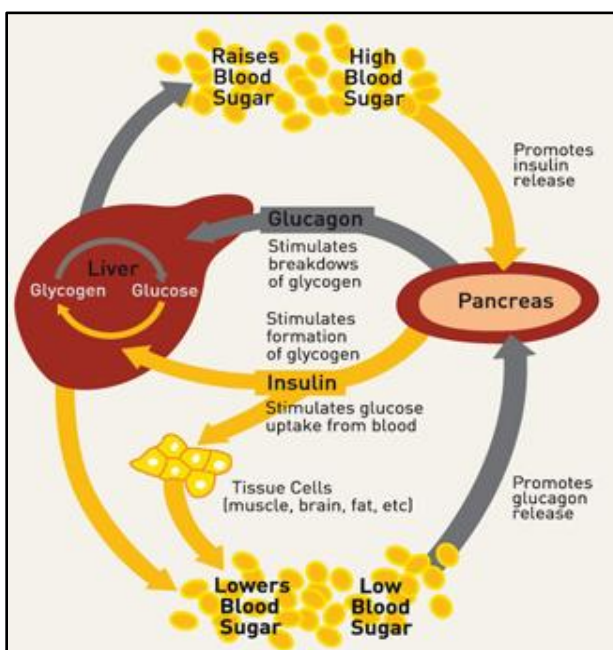


Figure 3: Insulin action

The main function of insulin consists in the regulation of glucose disposal in humans in order to maintain blood glucose levels between 3.8 and 6.1 mM in the fasting state (Figure 3). Once blood glucose levels reach about 5 mM, insulin release is provoked and the hormone is transferred into the blood circulation system through oscillation of the cell membranes.

Insulin affects metabolic actions within multiple organs and cell types. Increased insulin levels promote glucose uptake in muscle, brain and fat tissue cells. The liver is stimulated to form glucose storage and

creates glycogen. Glycogenolysis (degradation of stored glucose) and gluconeogenesis (synthesis of glucose) are inhibited. In adipocytes, insulin also has an anti-lipolytic effect, which means that it inhibits degradation of free fatty acids. During fasting periods, when insulin levels decrease, lipolysis is promoted to create energy and maintain blood-glucose levels.

Insulin receptor molecules are critical in insulin function. There are three different receptors that pro-

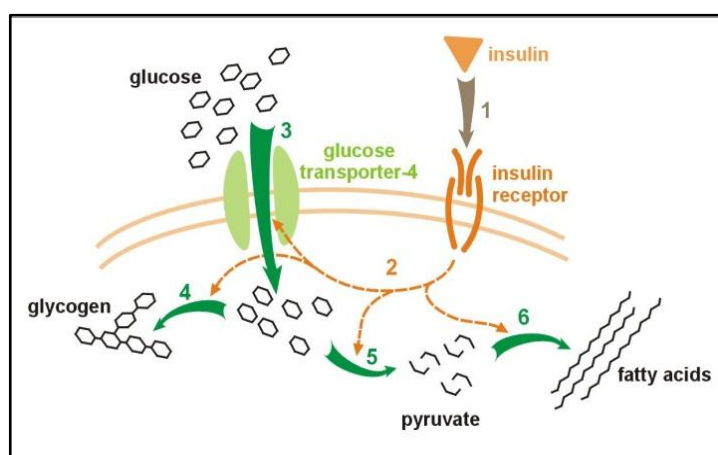


Figure 4: Insulin and glucose metabolism within the cell

mote the uptake of insulin and insulin-like growth factors into a cell, the insulin receptor (IR), the type 1 insulin-like growth factor (1 IGF)receptor and the type 2 IGF receptor. The insulin receptor is a large transmembrane glycoprotein that consists of two α - and two β -subunits. When insulin molecules bind to extracellular α -subunits they provoke conformational changes that lead to an approach of the α -subunits and enable ATP to bind to the intracellular domain of the β -subunits. A cascade of phosphorylation is activated and initiates different reactions within the cell.

Insulin released into the circulation can only bind to cells expressing the receptor on their plasma membranes. Almost all human cells express IR, but the level of expression varies greatly among different cell types. Above all, hepatocytes, adipocytes and myocytes are known to have the largest IR expression, amounting to several hundreds of thousands (Holt et al., 2010).

DM describes a category of metabolic disorders that result in hyperglycemia. The most common subtypes among the DM group are Type 1 DM and Type 2 DM (Figure 5). Type 1 DM is characterized by an autoimmune destruction of pancreatic β -cells followed by an insulin deficiency. Type 2 DM is characterized by insulin resistance, hyperinsulinemia and eventually by β -cell failure. In addition to Type 1 and Type 2, other types of DM can be caused by genetic defects, pancreatic disorders, drugs or pregnancy. The prevalence of DM has risen almost tenfold between 1985 and 2010. This corresponds to 285 million cases worldwide (Longo et al., 2012).

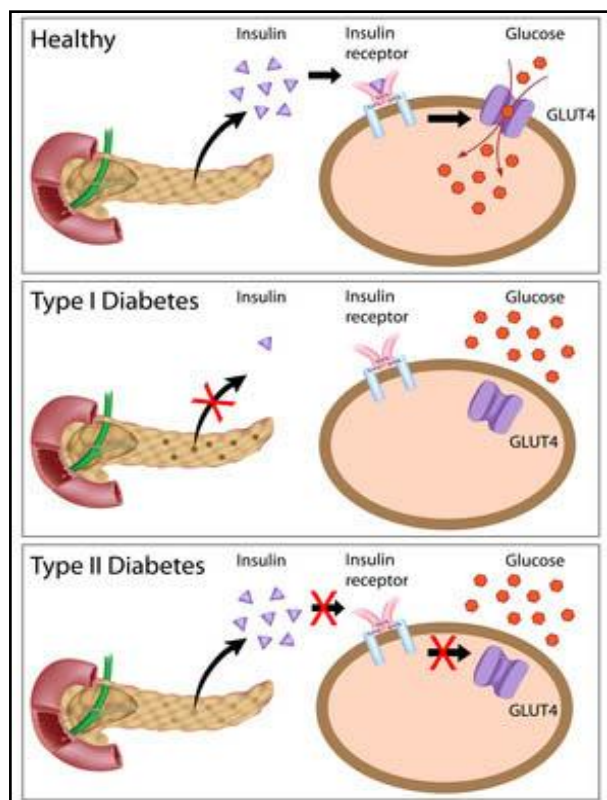


Figure 5: Type 1 and type 2 DM

Insulin resistance is a malfunction of insulin receptors and the intracellular insulin signaling pathway. Type 2 DM typically begins when high concentrations of free fatty acids in blood lead to a gradual insulin resistance in glucose-processing cells. Glucose, which is transported to cells via the blood circulation, can no longer be absorbed. It remains in the blood and leads to hyperglycemia. In response, pancreatic β -cells increase their insulin production in order to stimulate the glucose-processing cells to absorb more glucose. However, the elevated insulin level produces an aggravating effect: instead of taking more glucose in, the glucose-processing cells develop an insulin resistance as they lose sensitivity to the insulin.

Insulin resistance is an impairment of the signaling pathway between the insulin receptor on the cell surface and the activator of the GLUT glucose transporters, which allow glucose entry into the cell.

The interaction of decreased glucose uptake, hyperglycemia, increasing insulin levels and reduced glucose uptake defines a metabolic cycle that leads to symptoms such as tiredness, constant hunger and weight gain. After some time, the pancreatic β -cells begin to wear out and are no longer able to produce high levels of insulin. As they begin to die, insulin levels drop and consequently a deficit of insulin as well as hyperglycemia occurs.

Type 2 DM is a disease brought on by genetic and acquired factors. Studies have demonstrated that type 2 DM is prevalent in both twins in 91 % of all twins. Others have also shown that there are significant differences between various ethnic groups. In the U.S., 2 % to 4 % of Caucasians suffer from type 2 DM, whereas 40 % of all Pima Indians in Arizona are affected. In addition to genetic factors, lifestyle factors such as diet, exercise and obesity are also linked with type 2 DM. Obesity has the strongest effect on insulin resistance resulting in type 2 DM. Adipose tissue is associated with the production of proteins that decrease the ability of glucose processing cells to react to insulin. Therapeutic approaches for obese type 2 DM patients often suggest a change of diet with the addition of regular physical exercise to encourage weight-loss. In more progressed stages of the disease, medication-based treatment (glucosidase-inhibitors, insulin substitution) is required (Jameson et al., 2010).

2.2. Decidualization of endometrial cells

The maternal decidua is defined as part of the uterus that plays a crucial role when it comes to implantation of an embryo and the formation of the maternal placenta. It mainly consists of human endometrial stromal cells (HESCs). The process of differentiation, when normal HESCs differentiate into decidualized HESCs, is called decidualization.

2.2.1. Structure and function of the human endometrium

The human endometrium is one of three layers (parametrium, myometrium, endometrium) that build the uterine cavity. It consists of a multilayered mucosa which provides optimal conditions for implantation of an embryo and also for the general support of pregnancies (Lenz et al., 2012).

The structure of the human endometrium can be divided into two morphologically different layers. The upper two-thirds are called the functionalis (Figure 6). Its purpose is to prepare the uterus for a possible implantation of a blastocyst during the menstruation cycle. The functionalis is also the site of proliferation, secretion and degeneration of endometrial tissue. The

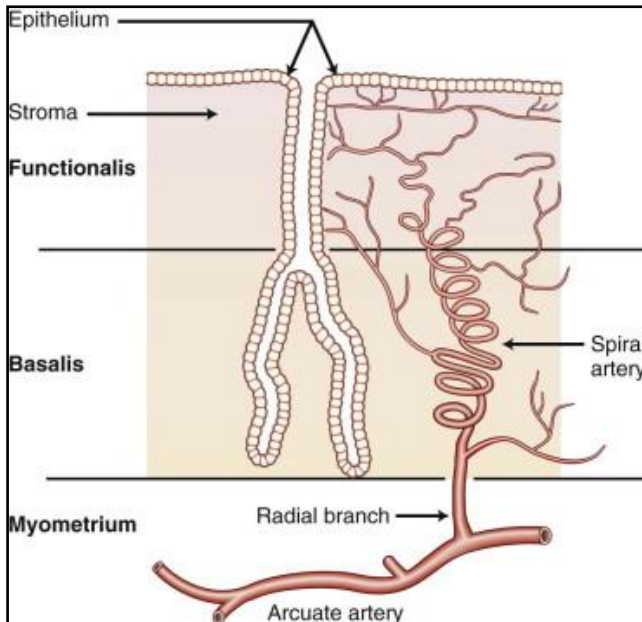


Figure 6: Functional anatomy of the human endometrium

lower third of the endometrium is the basalis layer (Fritz et al., 2011). Though the basalis does not change significantly throughout the menstrual cycle, it plays a crucial role in the regeneration of the endometrium tissue after the menstrual loss of functionalis (Hoffman et al., 2012).

The endometrium undergoes a periodic change during every menstrual cycle. Its structure differs depending on the phase it is in. At the beginning of the menstrual cycle, during menstruation, the endometrium is comparatively thin and dense. It consists of the stable basalis component and a strongly diminished functionalis

layer. Almost two-thirds of the functioning endometrium is shed. The tissue-loss is followed by a rapid repair; a new surface epithelium that covers the entire uterine cavity is rebuilt by day five to six (Figure 8).

After menstruation, at the proliferative phase, the human endometrium starts to reconstruct itself entirely. Due to the influence of estrogen, all tissue components such as stromal, glandular and epithelial cells begin to proliferate rapidly. Proliferation peaks at day eight to ten and at the end of the proliferative phase the endometrium grows from 0.5 mm to 3.5-5 mm.

When ovulation sets in, the endometrium transforms into a secretory tissue as a reaction to estrogen and progesterone activity. Glycogen-rich subnuclear vacuoles appear in cells near the endometrial glands. They then move towards the surface of the endometrium and begin to emit secretion. The secretory phase peaks around day six after ovulation, thereafter the glands appear exhausted and run dry. The upper layer of the endometrium starts to form tortuous and distended tissue with individual, sawtooth-like surfaces (Figure 7).

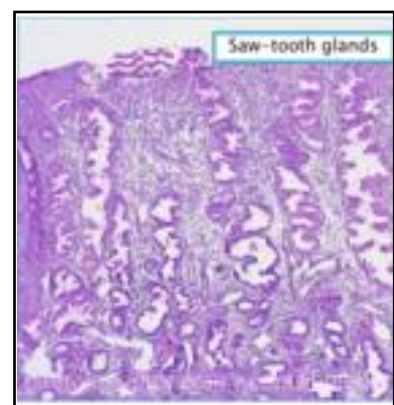


Figure 7: Endometrial tissue during secretory phase

After the secretory phase, the endometrium is ready for a blastocytes implantation. If this does not occur, the corpus luteum is not maintained by placental hCG and ceases to produce progesterone. As soon as the progesterone hormone levels begin to drop, the endometrial glands begin to collapse. Different components like incoming leukocytes, constricted spiral arteries and proteolytic enzymes induce tissue destruction.

At this point in the menstrual cycle, the period sets in and again sheds the entire functionalis leaving only the basalis layer to provide cells for endometrial regeneration (Hoffman et al., 2012; Fritz et al., 2011).

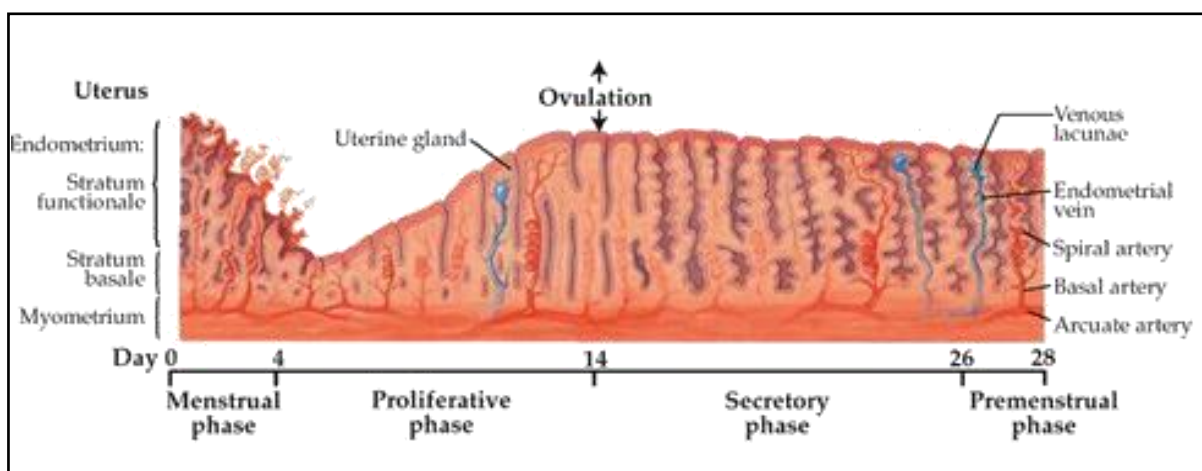


Figure 8: Endometrial transformation during the menstrual cycle

2.2.2. Decidualization of endometrial cells

During the secretory phase of the female menstrual cycle, endometrial stroma cells undergo a change of shape, structure and function (Figure 9). This process is called decidualization. It takes place in most mammals whose reproduction depends on the implantation of blastocyte into the uterine cavity. However, other than in most species, where decidualization is provoked by the blastocyte itself, decidualization in humans sets in across every menstrual cycle, independently of pregnancy. If fertilization occurs and implantation was successful, the human blastocyte promotes decidualization whereas it is aborted in case of an unfertilized oocyte (Gellersen et al., 2007).

For a long time, it was thought that decidualization was promoted by the post-ovulatory increased steroid hormone progesterone (Fritz et al., 2011). However, this assumption has been questioned during the last years: as progesterone increases about ten days before de-

decidualization starts, additional signals might be required to trigger its initiation (Gellersen et al., 2007).

According to Gellersen, decidualization begins in the terminal spiral arteries of the superficial endometrial layer and leads to a transformation of the spindle-shaped endometrial stromal cells into secretory, epithelioid-like decidualized cells (DCs). Throughout this process the cells' nuclei are rounding; their rough endoplasmic reticulum and their Golgi apparatus enlarge (Figure 9). Within the expanding cells, there is an accumulation of glycogen and lipid droplets. The extracellular matrix changes and establishes adherens junctions between stromal cells which lead to the formation of cuboidal morphology.

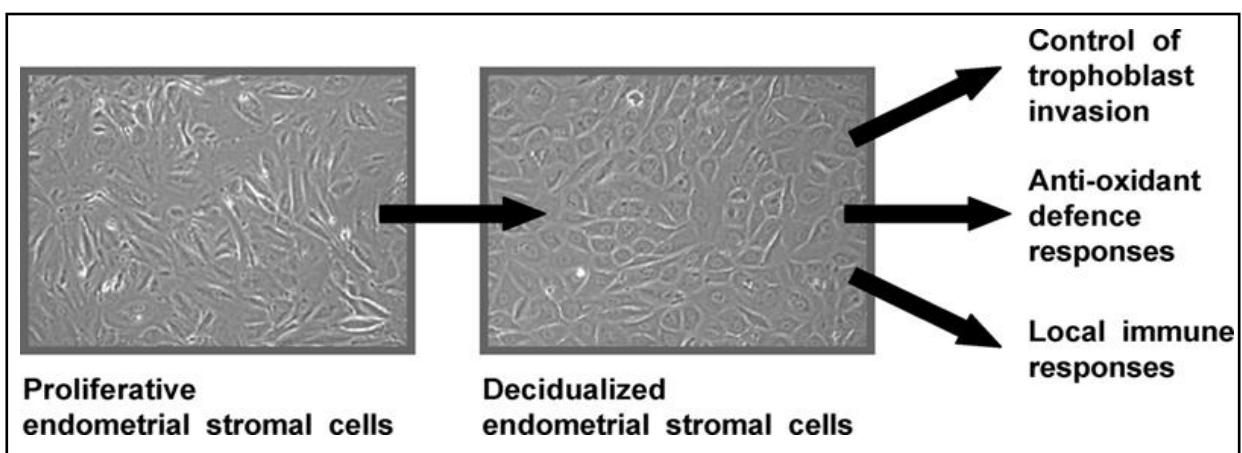


Figure 9: Changes of cell morphology during decidualization

As mentioned before, the endometrium is transformed into a secretory tissue during the secretory phase. DCs expel different products such as prolactin, insulin-like growth factor binding protein-1 and multiple cytokines. This transformation goes hand-in-hand with a process of genetic reprogramming involving genes responsible for cell adhesion, signal transduction, metabolism and stress responses (Gellersen et al., 2007).

Throughout the decidualization process, the human endometrium expands its functions and becomes capable of fulfilling three main tasks.

First of all DCs are able to control the trophoblasts invasion (Figure 10). Once the blastocyst has reached the uterine cavity, it starts to invade the maternal endometrium. The outer layer of the blastocyst is called the trophoblast. Decidualized stromal cells however create an ideal environment for the blastocyst attachment by secretion of cytokines

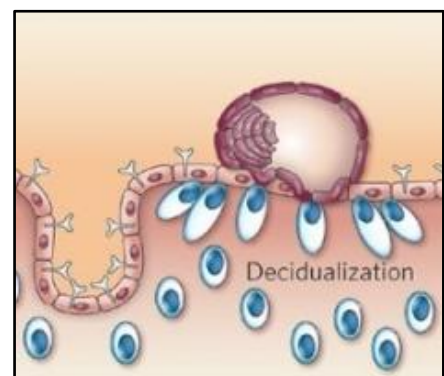


Figure 10: Implantation

and adhesive factors. They prevent the fertilized egg from burying itself too deeply into maternal tissue (Gellersen et al., 2007).

Secondly, decidualization supplies the blastocyst with oxygen and prevents its exposure to reactive oxygen species (ROS). ROS are byproducts of oxygen consumption and damage cell proteins, lipids and nucleic acids. They include superoxide anions, hydrogen peroxide and hydroxyl radicals. The trophoblast plugs to the spiral arteries of the endometrial tissue and connects the blastocyst with the maternal blood system. DCs respond to the increase in ROS levels by producing enzymes that are capable of neutralizing ROS and repairing or replacing damage (Thannickal, Fanburg. 2000).

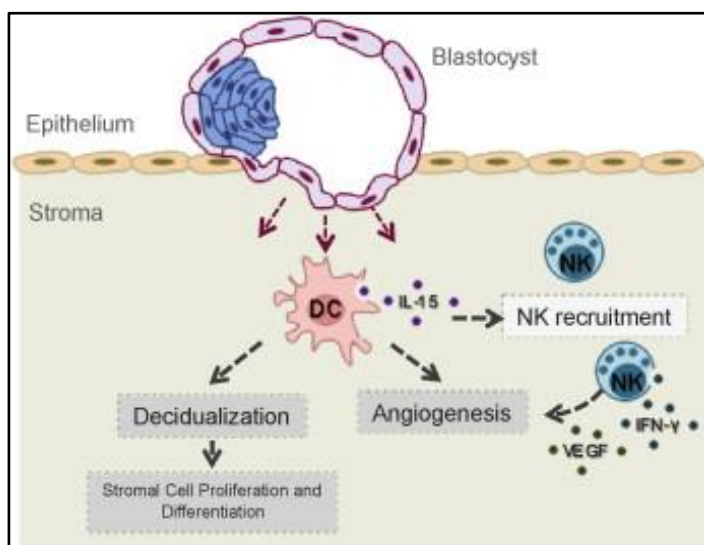


Figure 11: Trophoblast invasion and signaling

The third function performed by DCs is the inhibition of local immune responses in order to protect both the blastocyst and the mother (Figure 11). As the fetoplacental unit is formed by a semi-allogeneic tissue, the maternal immune system is likely to attack or reject it. Differentiated endometrial stromal cells have been proven to be involved in the recruitment of natural killer (NK) cells that are associated with the establishment of a tolerogenic environment.

NK cells that populate the locus of implantation inhibit T-cell proliferation and attenuate the expression of pro-inflammatory cytokines that are produced by activated T-cells (Koopman et al., 2003). Moreover, DCs produce enzymes such as indoleamine 2,3-dioxygenase (IDO), and transmembrane proteins such as Fas ligand, that suppress T-cell inflammatory responses or even induce apoptosis of activated T-cells.

2.2.3. Decidualization and infertility

Today, scientists estimate that about 30 % of all embryos are lost prior to implantation. Another 30 % do not overcome the first six weeks of gestation (Figure 12). It is widely presumed that such high rates of early pregnancy loss might be caused by both maternal and fetal factors. Conventional karyotyping experiments on lost embryonic tissue have shown that 30-60 % of all miscarriages are induced by chromosomal abnormalities of the concep-

tus. On the maternal side, multiple possible interference factors of immunological, anatomical, endocrine, or other nature can interfere with an ongoing pregnancy (Salker et al., 2010).

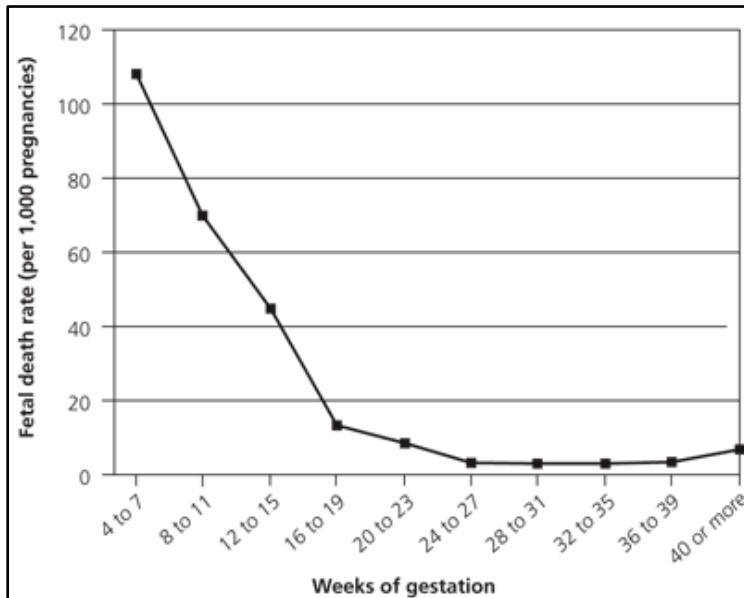


Figure 12: Estimated rates of fetal mortality by weeks of gestation

Pregnancy might be negatively affected by a nonfunctional decidualization process within the maternal body. The description of physiological decidualization suggests its tremendous importance for the positive progression of pregnancy. Without functioning DCs, both implantation and maternal-fetal communication might be compromised.

A malfunctioning endometrial environment often leads to reproductive complications such as recurrent pregnancy loss or infertility and may cause endometriosis (Guerin et al., 2009). While endometriosis may serve as an example of what happens if the physiological decidualization process is undermined by an exterior influence, a study has been performed to show the direct impact of impaired decidualization on early pregnancy loss rates. The group revealed that abnormal cyclic differentiation does lead to the increased expression of prokinectin-1, an enzyme that promotes implantation. If it is secreted beyond the average rate it prolongs the so-called window of implantation and boosts endometrial receptivity. This process impairs embryo selection and subsequently leads to a higher implantation rate of genetically compromised embryos, also resulting in higher rates of early pregnancy loss (Salker et al., 2010)

2.3. Correlation of insulin, decidualization and infertility

As demonstrated above, there is a strong correlation between the functional endometrial decidualization processes and positive pregnancy outcomes. Also, it has been indicated that decidualization may not only be induced by progesterone alone, but needs additional signals to be initiated (Gellersen et al., 2007).

To date, there have been several experiments that aimed to imitate the decidualization process *in vitro* in order to fully understand its physiology. In 1992, Gurdip et al. were suc-

successful at differentiating primary endometrial cells *in vitro* into DCs (Gurpide et al., 1992). The group used normal proliferative primary cells from biopsy material and a culture medium that contained medroxyprogesterone (MPA), the progesterone priming prostaglandine E₂ (PE) and insulin.

Positive decidualization outcomes were not only measured by the morphological changes of endometrial cells, but also by their secretion pattern: As endometrial cells decidualized, they begin to express the peptide hormone prolactin (PRL). Therefore, PRL is a commonly used decidualization marker (Gellersen et al., 2007)

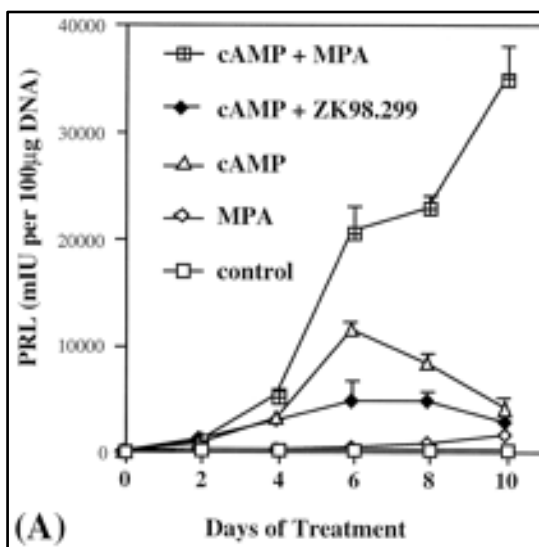


Figure 13: Impact of cAMP+MPA on decidualization by Brosens et al. (1999)

In 1999, Brosens et al. presented another model of *in vitro* decidualization (Figure 13). The highest outcome of fully decidualized cells could be achieved by a combined treatment of MPA and cyclic adenosine monophosphate (cAMP) (Brosens et al., 1999).

Recently, another research group, led by Dr. Mor of the Yale School of Medicines Department of Obstetrics and Gynecology created decidualized endometrial stromal cells by culturing them in a media containing E₂, MPA and OptiMEM (artificially manufactured cell culture medium). Within only eight days of cell culture they could perform a full decidualization process (unpublished data).

Interestingly, most of the here named culture media have one thing in common: They contain reagents that do not only promote decidualization, but are also linked to the above described peptide hormone insulin. Gurpide and also the Dr. Mor group added insulin directly into their media (the culture medium OptiMEM contains a large amount of insulin, in a range of 1720 to 2580 nM insulin as described by the manufacturer GIBCO and also by Kawamoto et al., 1983). Brosens et al. (1999) used substances that have a strong impact on the insulin signaling pathway (eg. cAMP promotes the expression of several kinds of insulin receptors (Ganef et al., 2008)).

2.3.1. Effects of insulin on fertility

The fact, that most of the protocols that aim at the decidualization of human endometrial cells contain insulin itself or insulin related factors, raises questions about the original role of insu-

lin within the human endometrium. Although there have been numerous studies on the insulin related insulin-growth-factor (IGF) family within the uterus (eg. Nayak, Giudice. 2003), hardly any experiments have been performed to reveal the insulin action itself.

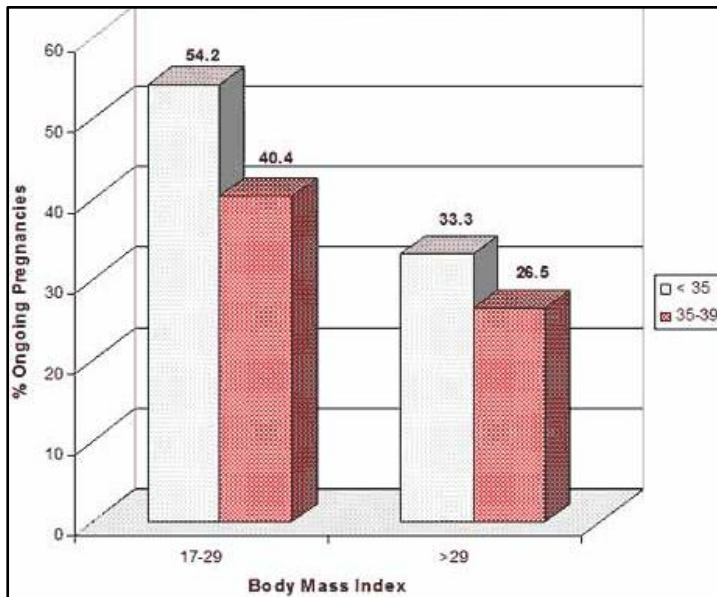


Figure 14: Pregnancy rates per stimulation by age and BMI

In addition, clinical data has shown that the prevalence for fertility disorders increases when pathologic levels of insulin come into play. As per Holt et al. (2010) obese women or women suffering from type 2 diabetes were found to have a threefold increase in recurrent early miscarriage, which is defined as more than three successive miscarriages before 12 weeks of pregnancy. Furthermore, the body mass index (BMI) has a significantly negative effect on success rates of fertility treatments (Figure 14).

Another disease pattern that links insulin to infertility may be illustrated by polycystic ovary syndrome (PCO). PCO occurs in almost 5-10 % of women in reproductive age and is defined by symptoms such as multiple ovarian cysts, abnormal estrous cycles and biochemical hyperandrogenism (= excess release of androgenic hormones). It leads to strongly decreased fecundability and fertility rates. Impaired glucose tolerance and insulin resistance have been discovered in almost 40 % of all PCO patients. At the same time, women suffering from PCO have a threefold higher risk of gestational diabetes (Holt et al., 2010).

2.3.2. Effects of insulin on decidualization – study design

Nowadays, the causes for significantly higher infertility rates in patients with hyperinsulinemia are still unknown. Possible effects of glucose and insulin metabolism for reproductive processes are various and complicated. Both glucose and insulin levels could directly impact the reproductive tract. They could also contribute to altered sex hormone production by influencing endocrine organs such as the pituitary gland or the thyroid (Brothers et al., 2010).

In order to contribute to ongoing research in the field of gynecology / endocrinology, this project investigated possible effects of glucose concentrations and insulin on endometrial stromal cells and decidualization processes.

The first aim of this study was to determine if human endometrial stromal cells (HESC) are sensitive toward different glucose levels and the presence/absence of insulin. Therefore, a growth study was performed: for one it compared the growth pattern of HESC in both high glucose and low glucose medium. In addition, growth of HESCs in high glucose medium plus 100 nM insulin was compared to low glucose medium plus 100 nM insulin. To obtain measurable growth curves, cells were counted at the start of the project, on day one, day three and day five. Additionally, pictures of cell growth were taken: in order to observe cells grow, culture plate wells were scratched (scraped). It was then monitored how quickly cells would grow back at different time points, using the same media.

As a second objective, this thesis aimed to mimic the decidualization process of HESCs *in vitro*. The basic model that was used was the already mentioned protocol of Dr. Gil Mor, associate of the Department of Obstetrics and Gynecology at the Yale School of Medicine. While Dr. Mors culture medium just contains E₂, MPA and OptiMEM, which is an artificial medium. Here, different experiments with different media were performed. There were various doses of insulin and also other ingredients, such as E₂ or MPA added or left out. At the same time, the development of HESCs in low glucose medium to high glucose medium was again compared. The decidualization project was performed over a period of eight days. On day one, day three, day six and day nine, pictures of cell morphology were taken and culture media were collected to perform ELISA and determine the level of PRL expressed by cultured cells. If decidualization were induced, they would be followed by increased levels of PRL. In addition, HESCs were collected after the protocol was finished and RNA was extracted in order to investigate whether the gene expression patterns followed the same patterns as those observed with the ELISA.

The hypothesis, which was to be verified in the course of those projects, is that HESCs are sensitive towards different glucose concentrations and insulin doses. Varying the concentrations of both of those substances will induce a significant difference when it comes to differentiation and proliferation capacities of HESCs.

3. Materials and methods

The following chapters describe the materials and methods that have been used in this bachelor project. The difficulty of the different methods and the handling of the cells made that some of the methods did not contribute to the data obtained. For reasons of completion, the methods have been described here nevertheless.

3.1. Materials

For both the growth curve and the decidualization project, primary HESCs were used that had been collected during surgeries performed at the Yale School of Medicine. The biopsy material belonged to three patients between 34 and 53 years of age and with a BMI range of 24 to 29. Biopsies were taken from their uteri in the course of clinical surgeries, such as laproscopies, hysterectomies or ovarian cysts. All patients were informed about study details and gave their written consent to cooperate.

3.2. Treatment plans

During the course of the studies, treatment plans were developed and further optimized. These plans are described in detail for the growth curve experiments and the decidualization protocol, since the treatment plans differed between these two experiments.

3.2.1. Growth Curve

- **Cell preparation**

Primary HESCs at passage 3 were trypsinized, harvested and plated onto four 12-well plates and also on one 6-well plate each at a concentration of 10^5 cells/ml. For the following eight hours, the cells were cultured in low glucose Dulbecco's Modified Eagle's Medium (DMEM) plus 10 % fetal bovine serum (FBS), adding 1 % of antibiotics (PenStrep and Ampho B) in order to let them attach to the plates surface. After eight hours, the medium was changed into no-glucose DMEM plus 1 % PenStrep, plus 1 % Ampho B to starve cells overnight. The next morning, cells were counted (time point day 0). From that point on, the low glucose part of the plate was being cultivated in a medium containing low glucose DMEM, plus 10 % FBS plus 1 % PenStrep, plus 1 % Ampho B. The high glucose part of the plate was being cultivated in a medium containing high glucose DMEM, 10 % FBS plus 1 % PenStrep, plus 1 %

Ampho B. For the insulin treatments group, 100 nM insulin was added to both low and high glucose DMEM. Cells of the 12-well plates were trypsinized and counted by haematocytometer at day zero, day one, day three and day five. Cells in the 6-well plate were scratched and pictures were taken at starting point, day one, day two and day three.

- **Treatment groups**

1. **Low glucose DMEM containing 1 g glucose / dl + 10 % FBS + 1 % PenStrep + Ampho B**
2. **High glucose containing DMEM 4.5 g glucose / dl + 10 % FBS + 1 % PenStrep + Ampho B**
3. **Low glucose DMEM + 10 % FBS + 100 nM Insulin + 1 % PenStrep + Ampho B**
4. **High glucose DMEM + 10 % FBS + 100 nM Insulin + 1 % PenStrep + Ampho B**

- **Treatment schedule**

	Low Glucose DMEM + 10 % FBS	High Glucose DMEM + 10 % FBS	Low High Glucose DMEM + 10 % FBS + 100 nM INSULIN	High Glucose DMEM + 10 % FBS + 100 nM INSULIN
Day -1	Plate cells in low glucose medium + 10% FBS, Let them attach to the plates surface for eight hours Switch medium into no-glucose DMEM to starve them over night			
Day 0	Switch to low glucose medium	Switch to high glucose medium	Switch to low glucose medium + insulin	Switch to high glucose medium + insulin
	Collect and count starting point cells Scratch 6-well plate, take pictures of starting point			
Day 1	Collect and count day one cells Take pictures of 6-well plate of day one cells			
Day 2	Take pictures of 6-well plate of day two cells			
Day 3	Collect and count day three cells Take pictures of 6-well plate of day three cells			
	Switch low glucose medium	Switch high glucose medium	Switch low glucose medium + insulin	Switch high glucose medium + insulin
Day 5	Collect and count day five cells			

3.2.2. Decidualization Project

- **Cell preparation**

Primary cells of two patients were extracted from biopsied material (for tissue extraction technique see below); they were then plated into two 12-well plates per sample (ergo four 12-well plates altogether) at a concentration of 5×10^5 cells per well and cultured at 37°C with 5 % CO_2 for five days until they reached a 100 % confluency (medium containing DMEM + 10 % FBS + 1 % PenStrep + 1 % Ampho B). Medium was then removed and individual media (Figure 15) were added. Note: Both high and low glucose media were phenol-red free DMEM and contained 1 % PenStrep and 1 % Ampho B.

For the following ELISA-analysis, media were collected and frozen at -20°C at specific time points (day one, day three, day six and day nine). In order to watch changes in cellular morphology, pictures were taken at the same days.

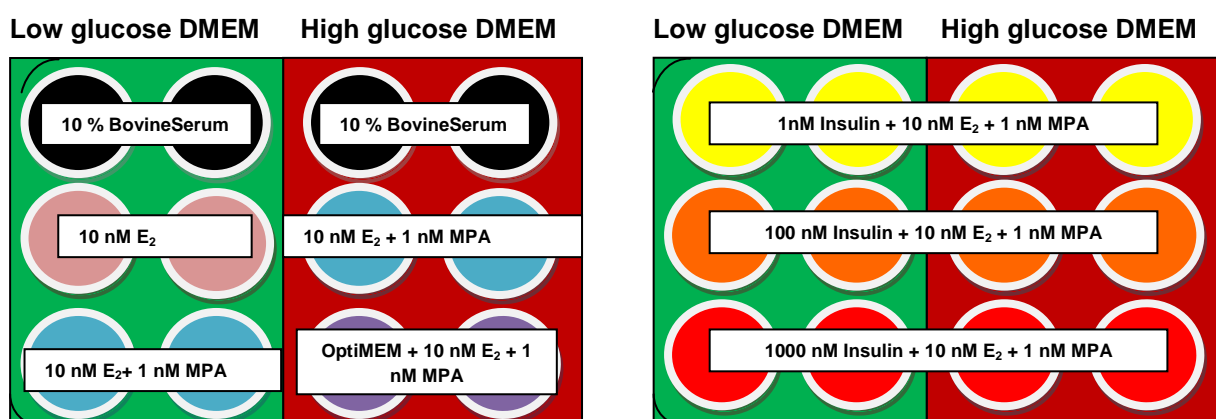


Figure 9: Plate design

- **Treatment groups**

1. Low glucose (1 g/dl) DMEM + 10 % FBS + 1 % PenStrep + Ampho B
2. Low glucose (1 g/dl) DMEM + 10 nM of E₂ + 1 % PenStrep + Ampho B
3. Low glucose (1 g/dl) DMEM + 10 nM of E₂ + 1 nM medroxyprogesterone (MPA) + 1 % PenStrep + Ampho B
4. High glucose (4.5 g/dl) DMEM + 10 % FBS + 1 % PenStrep + Ampho B

5. High glucose (4.5 g/dl) DMEM + 10 nM E₂ + 1 nM MPA + 1 % PenStrep + Ampho B
6. OptiMEM + 10 nM E₂ + 1 nM MPA
7. Low glucose (1 g/dl) DMEM + 1 nM Insulin + 10 nM E₂ + 1 nM MPA+ 1 % PenStrep + Ampho B
8. Low glucose (1 g/dl) DMEM + 100 nM Insulin + 10 nME₂ + 1 nM MPA+ 1 % PenStrep + Ampho B
9. Low glucose (1 g/dl) DMEM + 1000 nM Insulin + 10 nM E₂ + 1 nM MPA + 1 % PenStrep + Ampho B
10. High glucose (4.5 g/dl) DMEM + 1 nM Insulin + 10 nM E₂ + 1 nM MPA + 1 % PenStrep + Ampho B
11. High glucose (4.5 g/dl) DMEM + 100 nM Insulin + 10 nM E₂ + 1 nM MPA+ 1 % PenStrep + Ampho B
12. Low glucose (1 g/dl) DMEM + 1000 nM Insulin +10 nME₂ + 1 nM MPA+ 1 % PenStrep + Ampho B

- **Treatment schedule**

	Low Glucose DMEM + 10 % FBS	High Glucose DMEM + 10 % FBS
Day -1	Change medium into no-glucose medium in order to starve cells for 12 h	
Day 0	Change medium into treatment media. Take pictures.	
Day 1	Change treatment media. Collect media for ELISA. Take pictures.	
Day 3	Change treatment media. Collect media for ELISA. Take pictures.	
Day 6	Change treatment media. Collect media for ELISA. Take pictures.	
Day 9	Change treatment media. Collect media for ELISA. Take pictures. Collect cells for RNA extraction and RT-PCR	

- **ELISA-Analysis, mRNA extraction and qRT-PCR**

After all media had been collected, a sandwich ELISA was performed to determine the levels of prolactin (PRL) within the individual media (for ELISA technique see below). As mentioned before, PRL is a common marker for decidualization processes. Comparisons between the

different treatment groups should allow us to draw conclusions about the impact of different media on their differentiation processes. Also, HESCs were collected after the protocol was finished, mRNA was extracted and a qRT-PCR was performed (for mRNA extraction and qRT-PCR technique see below). This procedure aimed to show the gene expression pattern of eventually decidualized cells.

3.3. Laboratory techniques

The different laboratory techniques used for the cell isolation, cell culturing and the different analysis methods are described in the chapters below.

3.3.1. Cell culture

- **Cell digestion**

In order to process the biopsied material obtained from gynecological surgeries, an enzyme digestion of the tissue was performed. This procedure aimed to isolate individual endometrial stromal cells from the collagenous tissue without impairing their functionality or capacity to proliferate.

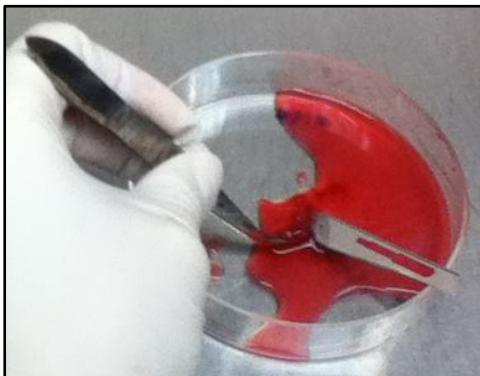


Figure 10: Cutting biopsy material with razor blade

As a first step, the tissue was scraped or poured into a petri dish and covered by 5 ml of enzyme digest. Enzyme digest consisted of 125 mg collagenase B (an enzyme that breaks peptide bonds within collagen tissues) 12.5 mg of DNase I, 150 ml of Hank's buffered salt solution (HBSS) and 1 ml PenStrep + 1 ml Ampho B. Using razor blades, the tissue sample was cut up into tiny pieces on the petri dish (Figure 16).

Once the tissue was sufficiently minced, the solution was transferred to a 50 ml colonial tube by using a pipette. The volume of the tube was filled to 15 ml of enzyme digest 5 ml HBSS was added. The solution was pipetted up and down for 20 times, then vortexed and incubated in the water bath at 37°C. Tissue was digested for at least 60 minutes, but vortexed every 5 minutes and pipette up and down with a 5 ml pipette 20 times every 15 minutes. After 60 minutes of enzyme digestion, cells were strained through a 40 μ M strainer directly into a 50 ml conical tube 5 ml at a time. This procedure was repeated once. The conical tube then contained en-

ometrial stromal cells. These could be transferred into culture flasks and be cultured in an incubator at 37 °C and 5 % CO₂.

- **Trypsinization**

When it comes to passaging adhesive cells to other containers or collecting them for other purposes (cell counts, cryo-preservations, etc.), cells need to be treated with the enzyme trypsin, so they detach from the surface of the container. Trypsin is a serine protease, which is originally produced as protrypsin within the pancreas of mammals. By reducing proteins it inhibits the cells adhesion capacity. Once treated with trypsin, adhesive cells round up and dislodge and can therefore be collected easily.

For trypsinization, trypsin, phosphate buffered saline (PBS) and FBS containing medium were warmed at 37°C in the water bath. Media was aspirated from culture flasks under the lamina air flow, and containers were washed with PBS in order to remove all media contents. Pre-warmed trypsin was mixed well and added on the containers, so that their surface was covered (Figure 17). Containers were then incubated for 5-10 minutes at 37°C / 5 % CO₂.



Figure 17: Covering well with trypsin

After incubation, the trypsin effect was checked under the microscope. If cells were not detached yet, the incubation time was prolonged. If cells were sufficiently detached, media containing FBS was added to inactivate the trypsin. The whole liquid was then collected in a conical tube and spun down at 3000 rpm for 3 minutes. Trypsin solution was aspirated and the cell pellet was reconstituted in medium or PBS (depending on intended purpose).

- **Plating cells**

For plating cells, trypsinized cells were reconstituted in an admeasured amount of low glucose medium + 10 % FBS + 1 % PenStrep + 1 % Ampho B and counted. Before adding the cell solution into the individual wells, a small amount of medium was placed in each well / flask, so that cells would distribute equally. Now, the cell suspension was pipetted into the wells. The total amount of medium in one well of a 6-well plate was 2 ml, whereas the total amount of medium in one well of a 12-well plate was 1 ml. After plating cells, the plates were put in the incubator at 37°C / 5 % CO₂ until they attached and / or reached the intended confluence.

- **Counting cells**

Especially for the growth curve experiment, it was necessary to count cells at regular intervals. For this procedure, trypsinized cells of each well were collected in an individual 10 ml conical tube. They were then spun down as described above, and afterwards reconstituted in a total amount of 250 μ l medium per tube.

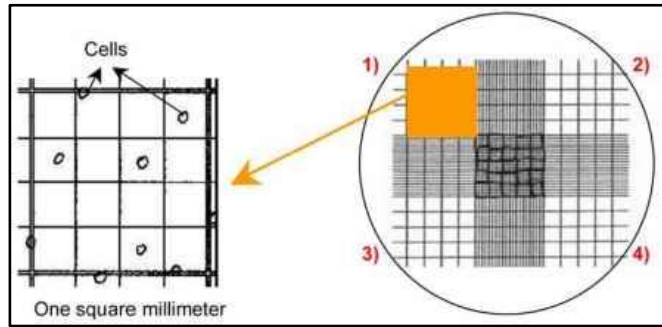


Figure 18: haemocytometer

At this point, it was crucial to mix the cell solution very well with an adequate pipette (we pipetted up and down for at least 20 times). After this, an amount of 10 μ l was taken out and injected into the small slot between haemocytometer and cover glass (Figure 18). Now, the haemocytometer was placed under the microscope and the focus was set on one of the 16 corner squares. Using a hand tally counter, the cells in this square were counted (only count live cells). This procedure was repeated with four different 16 corner squares. The haemocytometer is designed so that the number of cells in one set of 16 corner squares is equivalent to the number of cells $\times 10^4$ / ml.

3.3.2. ELISA

The enzyme-linked immunosorbent assay (ELISA) is a widely used immunochemical technique that aims to determine levels of specific antibodies or antigens in liquid samples. There are several different kinds of ELISAs, such as the indirect ELISA, the competitive ELISA or the sandwich ELISA. They all consist of the same principle: As a first step an antigen-antibody complex is formed, whereas one of those components – antigen or antibody – is found

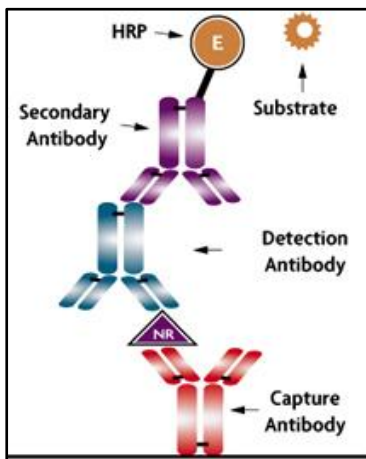


Figure 19: Antibody-antigen-antibody complex

in the analyzed sample. The second step includes binding of a detection antibody to the antigen-antibody complex and its detection via fluorescence absorbance (Figure 19; Burtis et al., 2012).

In this thesis, a sandwich ELISA was used to detect levels of PRL in the media of the decidualization experiment groups. The name “sandwich ELISA” describes the method's principle to form an antibody-antigen-antibody complex: the first antibody (capture antibody) is bound to the plate's surface and the antigens are contained within the applied sample. A secondary en-

zyme-linked antibody (detection antibody) is then added.

The advantage of sandwich ELISAs lies in both its simplicity and in its efficiency: as the antigen does bind to the specific capture antibody, there is no need for any purifications steps before analysis. At the same time, the specific binding increases both specificity and sensitivity of the assay (<http://www.elisa-antibody.com/>). In order to follow the corresponding protocol, the following steps were performed (Figure 20):

1. A specific ELISA plate was coated with 100 μ l of PRL capture antibody (concentration 400 ng/ μ l) per well. The plate was then incubated over night at 4°C. The day after, three washing steps with 390 μ l of wash buffer followed to eliminate unbound capture antibody. For washing, the plate was put on a shaker for 10 minutes per step. As a next step, all nonspecific binding sites of the capture antibody were blocked with 300 μ l of reagent diluent by incubating the plate during one hour on the shaker. After that, three washing step performed as described above, were performed.
2. Thereafter, antigen containing samples were added onto the coated wells. 100 μ l of the before collected medium were added, whereat different media from different time points and different experiment groups were used. Also, a standard curve, using 100 μ l of PRL standards with concentrations of 1000 pg/ml, 500 pg/ml, 250 pg/ml, 125 pg/ μ l, 62.5 pg/ml, 31.25 pg/ml and 15.625 pg/ml was performed. The plate was covered and incubated on the shaker for two hours. After that, three washing steps followed to wash away all samples that had not bound to the capture antibody on the plate surface.
3. In a third step, 100 μ l of secondary PRL-specific detection antibody (concentration 0.8 μ g/ml) was applied to bind to the already existing antigen-antibody complex in the wells. The plate was covered and incubated on the shaker for two hours. After that, three washing steps followed to remove all unbound detection antibody.
4. Now, 100 μ l of diluted Streptavidin-HRP, dilution 1:200, were added. HRP-conjugated Streptavidin is a protein that is bound to the enzyme horseradish peroxidase (HRP), which on the other hand provides enzyme activity for detection if it binds to the biotin region of the before applied detection antibody. The plate was then incubated for 20 minutes in the dark and afterwards washed three times.

- 100 μl of substrate solution were added per well in order to catalyze the HRPs enzyme activity, the ELISA plate was therefore incubated for 20 minutes in the dark. After that, the solution had developed a blue color. Finally, 50 μl of stop solution was applied to each well, to cut the reaction. Now, an absorbance measurement at 450 nm was performed to determine the levels of PRL that were contained in the different wells.

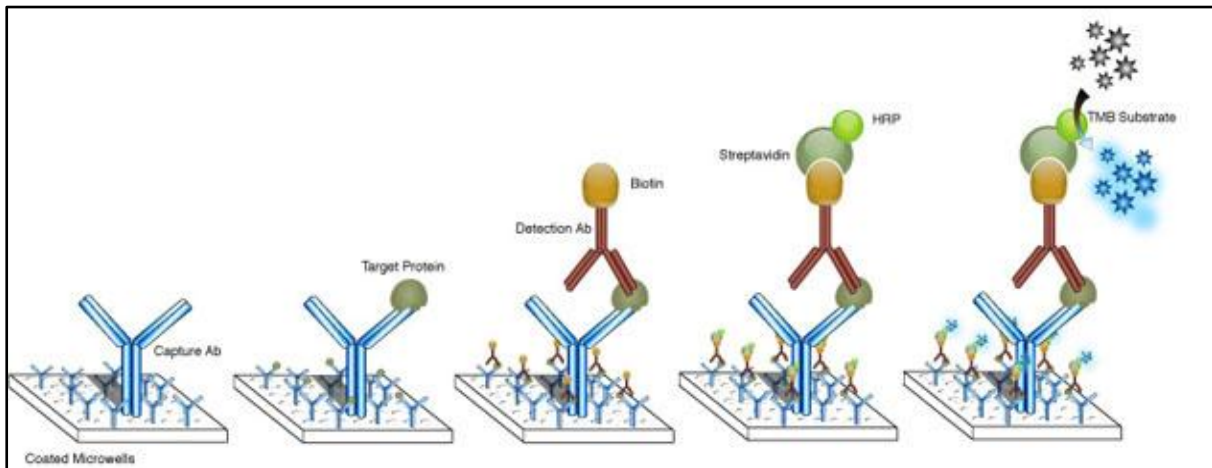


Figure 20: Sandwich ELISA

3.3.3. mRNA extraction, formation of cDNA and qRT-PCR

In order to determine cell activity and cell development, it is advantageous to analyze the gene expression levels in the cells after hormonal treatment. A way to do so is by extracting messenger ribonucleic acid (mRNA) and then converting it into complementary deoxyribonucleic acid (cDNA). cDNA is used as a template to perform quantitative reverse transcriptase polymerase chain reaction (qRT-PCR). In this case, the realization of those working steps aimed to follow possible changes regarding expression of PRL markers during the differentiation process of endometrial stromal cells.

- mRNA**

mRNA is generated in the cell nucleus and leads to protein biosynthesis. Its purpose is not only to copy genetic information from the DNA but also to transport it to the ribosome, where the actual formation of proteins happen (Figure 21). mRNA, as well as other kinds of RNAs, such as

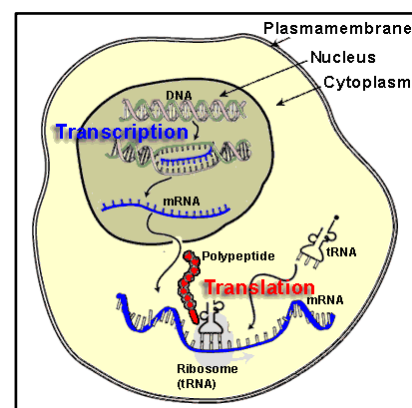


Figure 11: Schema of Transcription

tRNA, rRNA, etc.) is formed during transcription. This process is defined by the transformation of double stranded DNA (consisting of the four adenin [A],guanine [G],cytosin [C] and thymin [T] into single stranded RNA (consisting of A,G,C and U, as the base thymin is replaced with uracil [U]). Transcription is initiated by an enzyme called the RNA polymerase.

The value of mRNA for research purposes and diagnostic analysis lies mainly in its correspondence to gene expression. mRNA can only be produced under the condition of active gene expression, which means that only exons (=active gene regions) can be copied; inactive genes or gen regions (such as introns) are not being transcribed into any kind of RNA. As a consequence, mRNA patterns can give certain information about a cells nature, its activity and its environment (Alberts et al., 2008).

- **mRNA extraction**

Before mRNA can be processed, there is a need to extract it from the cell's nucleus and isolate it from all other components, which could interfere with the analysis results (proteins, lipids, carbohydrates etc.). Nowadays, there are several different methods of mRNA extraction, the one that was used in the here presented experiment is provided by Qiagen Sample & Assay Technologies (Figure 22).

The principle of the Qiagen's RNA purification kit involves selective binding properties of a silica-based membrane with the speed of microspin technology. At first, cell samples were lysed and homogenized with help of 350 µl highly denaturing guanidine-thiocyanate-containing buffer (RLT buffer) per well of a 12-well plate. The RLT buffer ensures the inactivation of RNases in order to guarantee purification of intact RNA. After that, 350 µl of 70 % ethanol were added to establish ideal binding conditions. The homogenized samples were applied to the RNeasy Mini spin column, where total RNA bound to the membrane. The spin column was placed in the centrifuge and the solution was spun down at 10 000

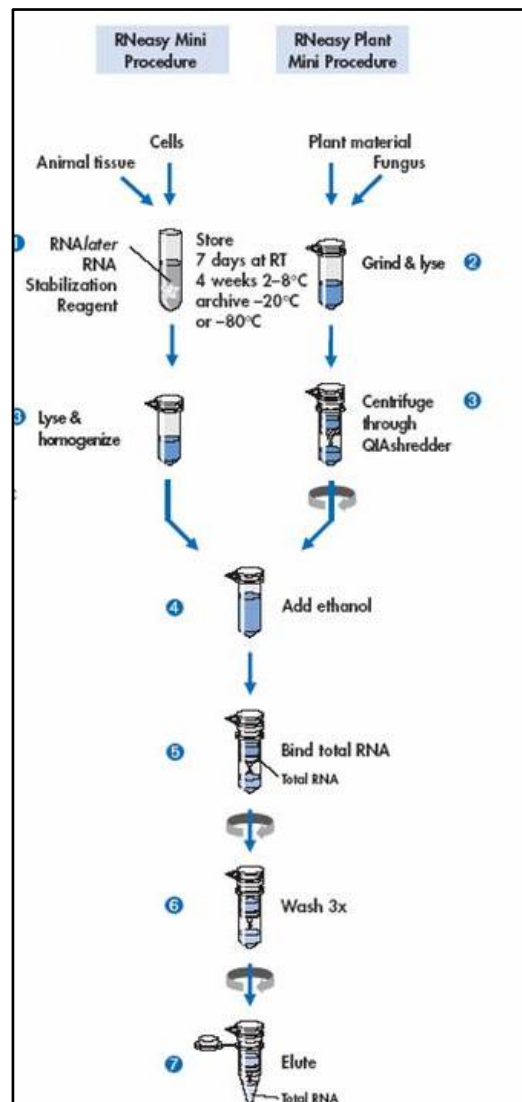


Figure 22: Qiagen's short protocol for RNA extraction

rpm for 15 seconds. After that, three other centrifuge steps (2 times 15 seconds and 1 time

2-5 minutes at 10 000 rpm) were performed, while there were always 500 µl of wash solution (RPE Buffer) added in between. Finally, one last centrifugation step followed (1 minute at 10 000 rpm), but this time no RPE buffer was added. As a last step, the isolated RNA was being eluted with 30 µl water and the whole RNA was spun down (1 minute at 10 000 rpm) into a 1.5 ml eppendorf tube for final collection (RNeasy® Mini Handbook, 2010).

The reason, why above all different kinds of RNA, mRNA is the one targeted by the Qiagen method, is its capacity to act as a template for complementary DNA (cDNA).

- **cDNA**

cDNA is a type of DNA, which is artificially synthesized by an enzyme called reverse transcriptase (Figure 23). As the use of RNA for molecular biological methods is limited due to its single stranded structure and its lack of stability, the creation of cDNA makes it possible to perform those methods nonetheless. The process of cDNA synthesis has some resemblance to the steps of a typical polymerase chain reactions (PCR, see below), but as RNA is already single stranded, there is no need for a denaturation step. This is why at first an oligo-dT primer is used for hybridization. By adding correspondent nucleotides, the reverse transcriptase enzyme is starting to build a complementary strand to the mRNA template. In the following process, this first cDNA strand will act as a template for the amplification of other, identical cDNA strands led by a normal DNA-polymerase. The original mRNA strand is meanwhile degenerated by another enzyme called RNase H (Lodish et al., 2013).

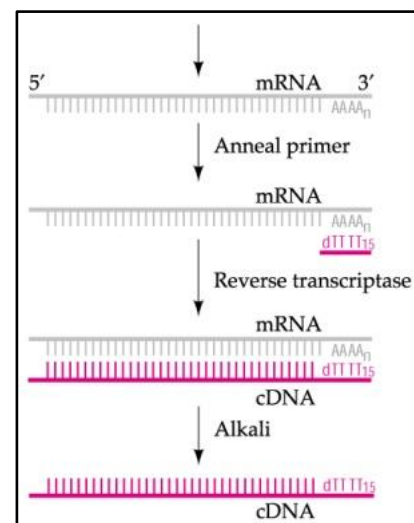


Figure 23: Synthesis of cDNA

For the here performed cDNA assay, an iScriptcDNA Synthesis Kit from Biorad was used. The components of each PCR-tube respectively the reaction protocol were the following:

4 µl 5x iScript reaction mix 4	5 minutes at 25°C
1 µl iScript reverse transcriptase	30 minutes at 42°C
X µl of RNA (concentration 500 ng/µl)	5 minutes at 85°C
15 – X µl of Nuclease-free water	Hold at 4°C (optional)
Total volume: 20 µl	Total time: 40 minutes

After cDNA synthesis was finished, it was diluted 1:20 and then processed via qRT-PCR.

- **qRT-PCR**

Quantitative realtime polymerase chain reaction (qRT-PCR) is a nucleic acid amplification method, which aims to amplify ribonucleic acid (RNA) targets. As originally described, this technique allows determining gene expression within a cell at a specific point in time and is therefore particularly suitable for the surveillances of cell developments and differentiation processes.

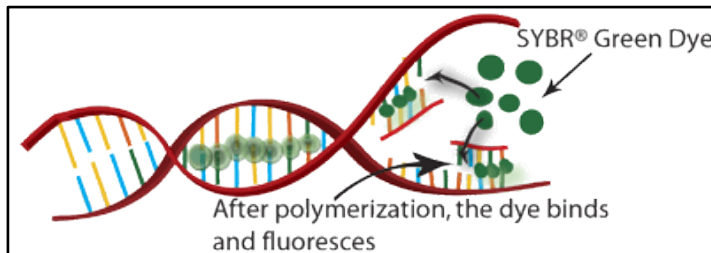


Figure 24: SYBRgreen action during qRT-PCR

qRT-PCRs consists of all steps of a conventional PCR (denaturation, hybridization, elongation), yet instead of DNA, artificially produced cDNA serves as template. Also, qRT-PCR operates with a nucleic acid stain such as SYBRgreen that

binds to double stranded DNA. It helps to measure the quantity of amplified DNA as it emits green light which can be detected and calculated in real-time during each PCR-cycle (Figure 24; McPherson et al., 2011)

The purpose of the here performed qRT-PCR was to determine the gene expression pattern of PRL after decidualization treatment. A iQIscript™ One-Step RT-PCR Kit with SYBR® Green that contained all RT-PCR components such iScript reverse transcriptase, 2x SYBR® Green RT-PCR reaction mix and nuclease-free water was used. As for the primers, both actin and PRL primers were included along the amplification process. The composition of ingredients in each PCR-tube and qRT-PCR protocol was the following:

12.5 µl SYBR® Green RT-PCR reaction mix (including iScript reverse transcriptase)	Cycle 1: (1x) Step 1: 95.0°C for 03:00
5.5 µl Nuclease free water	Cycle 2: (40x) Step 1: 95.0°C for 00:15
1 µl Actin OR PRL forward primer	Step 2: 60.0°C for 00:20
1 µl Actin OR PRL reverse primer	Step 3: 72.0°C for 00:25
5 µl cDNA (concentration 100 ng/µl)	Cycle 3: (1x) Step 1: 95.0°C for 01:00
Total volume: 25 µl	Cycle 4: (1x) Step 1: 55.0°C for 01:00
	Cycle 5: (80x) Step 1: 55.0°C for 00:10
	Cycle 6: (1x) Step 1: 4.0°C HOLD
	Total time: 2 h 6 minutes

Primers had been previously purchased at Primer-BLAST designed tools. Their sequences were:

Actin sense primer: 5'-CGTACCACTGGCATCGTGAT-3'

Actin antisense primer: 5'-GTGTTGGCGTACAGGTCTTTG-3'

Prolactin sense primer: 5'-CGCCATGGAAAGGGTCCCTCCT-3'

Prolactin antisense primer: 5'-CGCCGGGACAGATGGGCAAG-3'

After finishing the qRT-PCR the results were collected and analyzed. The ΔC_t values were calculated. C_t , also known as cycle threshold, defines the value that shows the first significant increase of fluorescence across a PCR protocol. ΔC_t is the difference between C_t value of the investigated gene expression (in this case PRL) and an intern control (actin). Its calculation is performed by subtracting a samples' PRL C_t from its actin C_t . Results indicate the fold change between control and the samples gene expression.

4. Results

4.1. Growth curve

Altogether, four different growth curves (n=4) were performed. Two of them compared the cell growth of HESCs in low glucose medium and high glucose medium (plus 10 % FBS and 1 % PenStrep / 1 % Ampho B in each). The other two expanded this protocol with an addition of low glucose medium plus 100 nM insulin, and high glucose medium plus 100 nM insulin (plus 10 % FBS and 1 % PenStrep / 1 % Ampho B in each). Cells were counted at day 0, day one, day three and day five (for raw data see appendix).

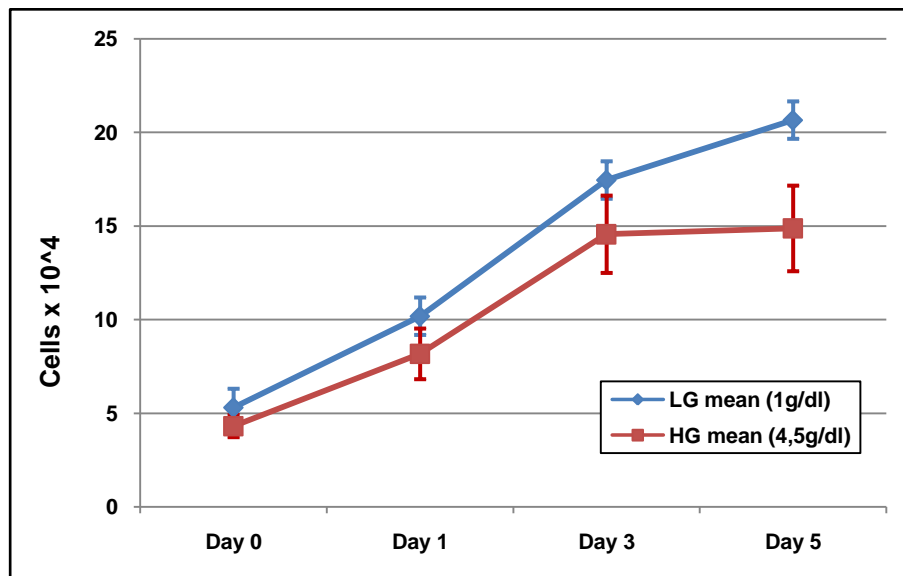


Figure 25: Growth curves: comparison of low and high glucose. Cumulative data of four separate experiments in primary ESCs, with each experiment completed in duplicate. Data show mean value +/- standard error of mean (SEM)

As seen in Figure 25, the growth curve did show a different growth pattern of HESCs in high glucose and low glucose medium. Though these results were not significant ($p = 0.13$ on day five), an obvious trend is visible: cells in low glucose medium continue to proliferate, whereas cells cultured in high glucose plateau in their growth on day 3. These findings may be underlined by the fact, that low glucose medium contains a glucose concentration of 1 g/dl, which corresponds to a level of 5.56 mM (Low glucose DMEM, www.invitrogen.com). This level of glucose mimics the physiological levels of human blood glucose which are between 3.8 and 6.1 mM in the fasting state (Holt et al., 2010). High glucose media however contains 4.5 g/dl, or 25 mM of glucose (High glucose DMEM, www.invitrogen.com). This glucose level is in the range of diabetic ketoacidosis, a pathological clinical state that may be fatal.

The second experimental series aimed at expanding the existing protocol with the addition of insulin to the treatment groups. Here, cells were treated with low glucose medium, high glucose medium, low glucose medium plus 100 nM insulin and high glucose plus 100 nM insulin.

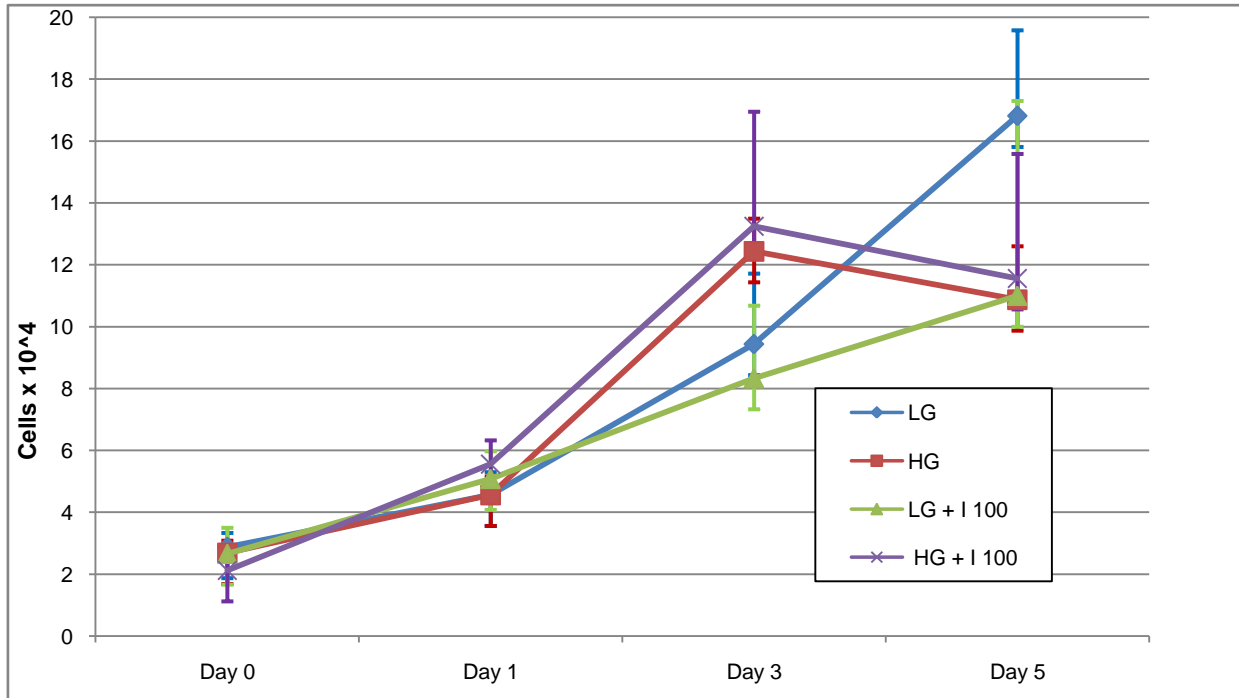


Figure 26: Growth curves: comparison of cell growth in media containing low glucose (LG), low glucose plus 100 nM insulin (LG + I 100), high glucose (HG) and high glucose plus 100 nM insulin (HG + I 100), in primary endometrial cells. Data are representative of two separate experiments, each in duplicate. Data show mean values +/- SEM

The trend that had been observed across the first growth curve could be reproduced in the second one: again, cell culture in low glucose medium resulted in an increased cell number compared to cells grown in high glucose medium (Figure 26). This time, the difference on day five with respect to the cell counts was significant ($p = 0.01$). While cells in low glucose medium seemed to grow constantly, cell growth in high glucose medium was characterized by a rapid growth of cells during the period of day one today three followed by stagnation or even decreasing cell numbers.

Other than expected, there was no further increase of cell growth achieved by adding a 100 nM insulin dose to any of the media: although the growth curve of high glucose plus 100 nM insulin mimicked cells growth in high glucose medium by augmenting cell growth very steeply during the first three days, it seemed to reach a plateau or even to decrease between day three and day five. Cell counts in low glucose media plus 100 nM insulin on the other hand stayed constantly low.

In summary, the data obtained across these two growth curve projects suggested that glucose concentrations, other than insulin - might have a large effect on cell growth.

4.2. Decidualization project

As part of the decidualization project PRL secretion by HESCs was analyzed by ELISA. In addition, alterations in the mRNA expression of PRL were determined by quantitative real time PCR.

4.2.1. ELISA analysis

Unfortunately, cell culture success was impaired by a large number of apoptotic cells across the eight day protocol of all decidualization cycles performed. Although all media at the designed time points had been collected, ELISAs could not be done since the number of cells still vivid at the end of the project had decreased significantly, the PRL levels measured could not be set in proportion to the cell number plated at the starting point and therefore lost their significance. These data could therefore not be used for this study.

4.2.2. qRT-PCR

As a consequence, another method was chosen in order to guarantee a more suitable approach: across the qRT-PCR protocol, all samples were processed with the same amount of RNA template (100 ng). This procedure aimed at obtaining comparable and standardized results, independently of changing cell counts or apoptosis throughout the culturing process.

In order to analyze all given samples, three plates of qRT-PCR were set up, and every sample was processed in triplicates (plate 1) or duplicates (plate 2 and 3) for internal control reasons (for raw data see appendix). The data obtained showed consistency in almost all numbers, only two samples had to be excluded because of inconsistency (sample # 153b I 100 / HG) or primer dimers (sample # 153b 10 % FBS/HG).

qRT-PCR amplification results showed very varying results: As seen in Figure 28, levels of prolactin expression had changed massively in some of the treatment groups: Compared to the control groups (10 % FBS/LG respectively 10 % FBS/HG) average fold changes in a range of 3fold change ($E_2+MPA+I100$ nM) to 1963 fold change (I 1000 nM / HG) were measured. A closer investigation of the obtained data led to the following conclusions: For one, the

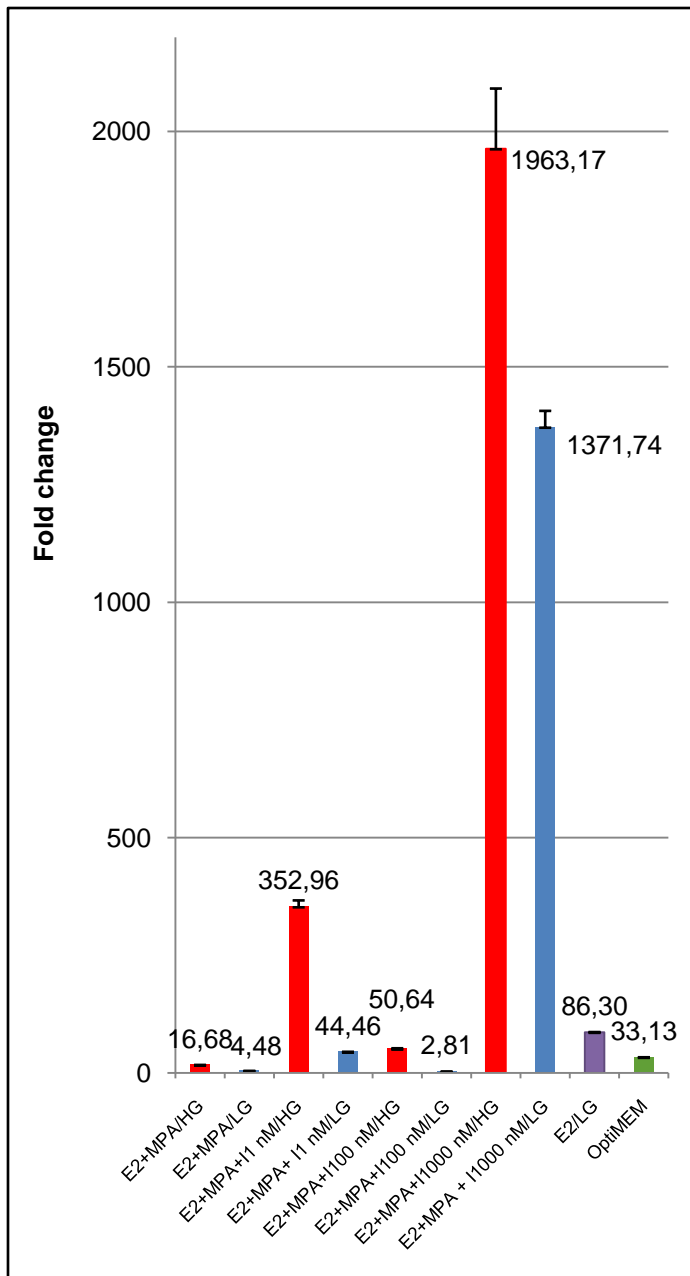


Figure 27: Fold change in prolactin expression in different treatment groups after 8 days of decidualization treatment. Data show mean value +/- SEM

data suggested that there was a difference in prolactin expression pattern between treatment groups cultured in low glucose and high glucose media: although low glucose groups showed multiple fold changes of prolactin expression too, they could not reach the expression levels of prolactin that high glucose groups did. Secondly, the house keeping gene actin seems to play a crucial role for the high measurements, as its levels were not as stable as expected

- **Low glucose / high glucose**

While the above described growth curve aimed to investigate if HESCs show an improved growth development in either high or low glucose medium, data obtained of the decidualization protocols might allow some conclusions concerning their differentiation abilities. The findings suggest that treatment groups cultured in high glucose (marked red in Figure 27) tend to express a greatly increased number of prolactin compared to cells treated with low glucose medium (marked blue in Figure 27). However, qRT-PCR results have also led to rather heterogeneous outcomes with high SEMs (+ SEM, see appendix for qRT-PCR data). Therefore, statistical comparison between high glucose and low glucose groups did not lead to significant p-values. Still, the assumption that high glucose medium may impair cell growth while it does boost cell differentiation at the same time is of great value and should be reviewed.

- **Actin / Prolactin**

Figure 27 clearly shows that prolactin expression differs widely between individual treatment groups. However, a closer look at the qRT-PCR data revealed that those measurements did not only result from alternating prolactin levels. Instead, the housekeeping gene actin may play a crucial role: while the prolactin expression stays relatively stable across all treatment groups (Figure 28), the actin expression changes significantly. As ΔCt values are defined as the exponential difference between levels of prolactin and actin, an unstable housekeeping gene naturally leads to big variations of calculated results.

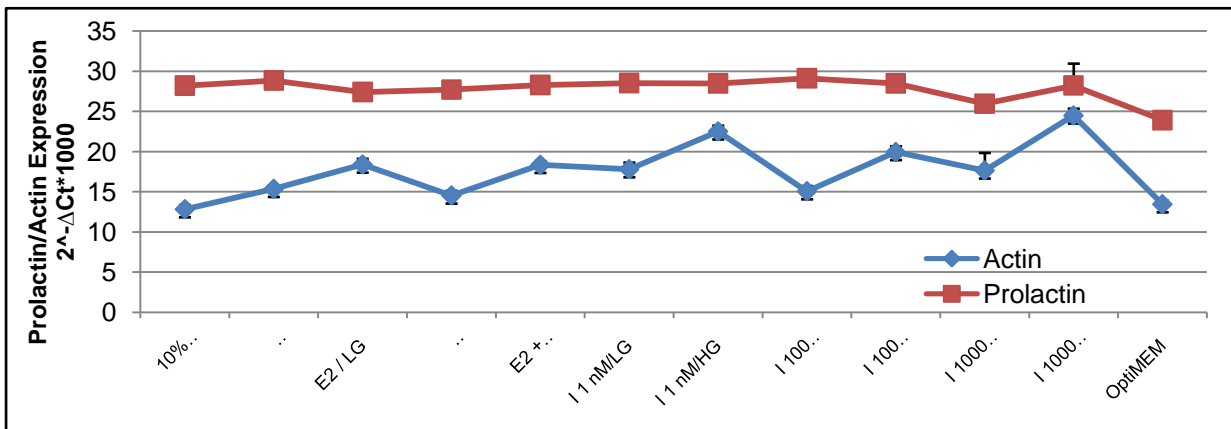


Figure 28: Actin expression vs. prolactin expression. Data show mean value +/- SEM

It has been reported earlier, that actin may not be an adequate housekeeping gene for all qRT-PCR. Amongst others, Lin and Redies (2012) put actin's value for normalization of gene expression in question when they reported in 2012, that its expression varies depending on type of tissue examined, experimental condition and developmental stages of cell material.

In case of the present decidualization project, there are two main assumptions of why actin levels vary across so strongly across different treatment groups:

A first pattern has been found when it comes to the correlations of actin levels in low glucose group vs. actin levels in high glucose groups (Figure 29). Here again, actin seems to be expressed at a much lower rate when cells are cultured in high glucose media, as it takes the melting curves of high glucose samples a larger number of cycles to cross cycle thresholds

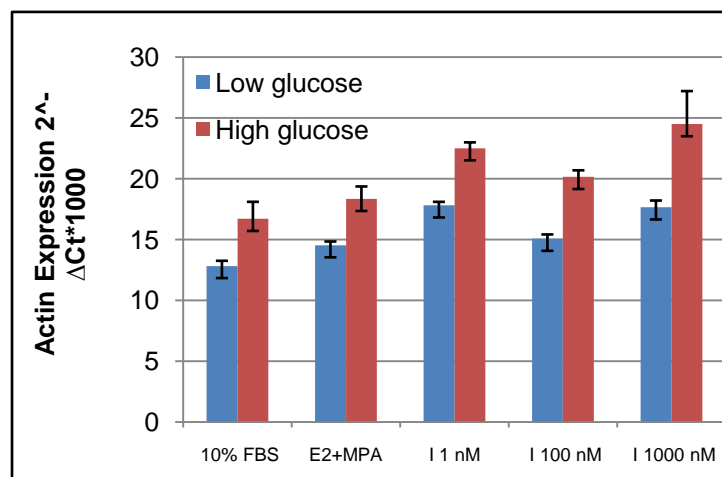


Figure 29: Actin expression in low glucose vs. high. Data show mean value +/-SEM

(CT). This observation leads to the hypothesis that cells cultured in high glucose medium may differentiate easier and therefore change their gene expression pattern earlier and more expansively than low glucose treatment groups.

A second possible explanation for unstable actin levels may be found within the cell culture process itself: As it has been mentioned before, a vast amount of cell death occurred during the decidualization process. Interestingly, the peaks within the actin expression curve correlate with cell groups where cell death was experienced most intensely (see Figure 30). This leads to the assumption that cell death cause changes within the cytoskeleton of dying cells and/or their gene expression.

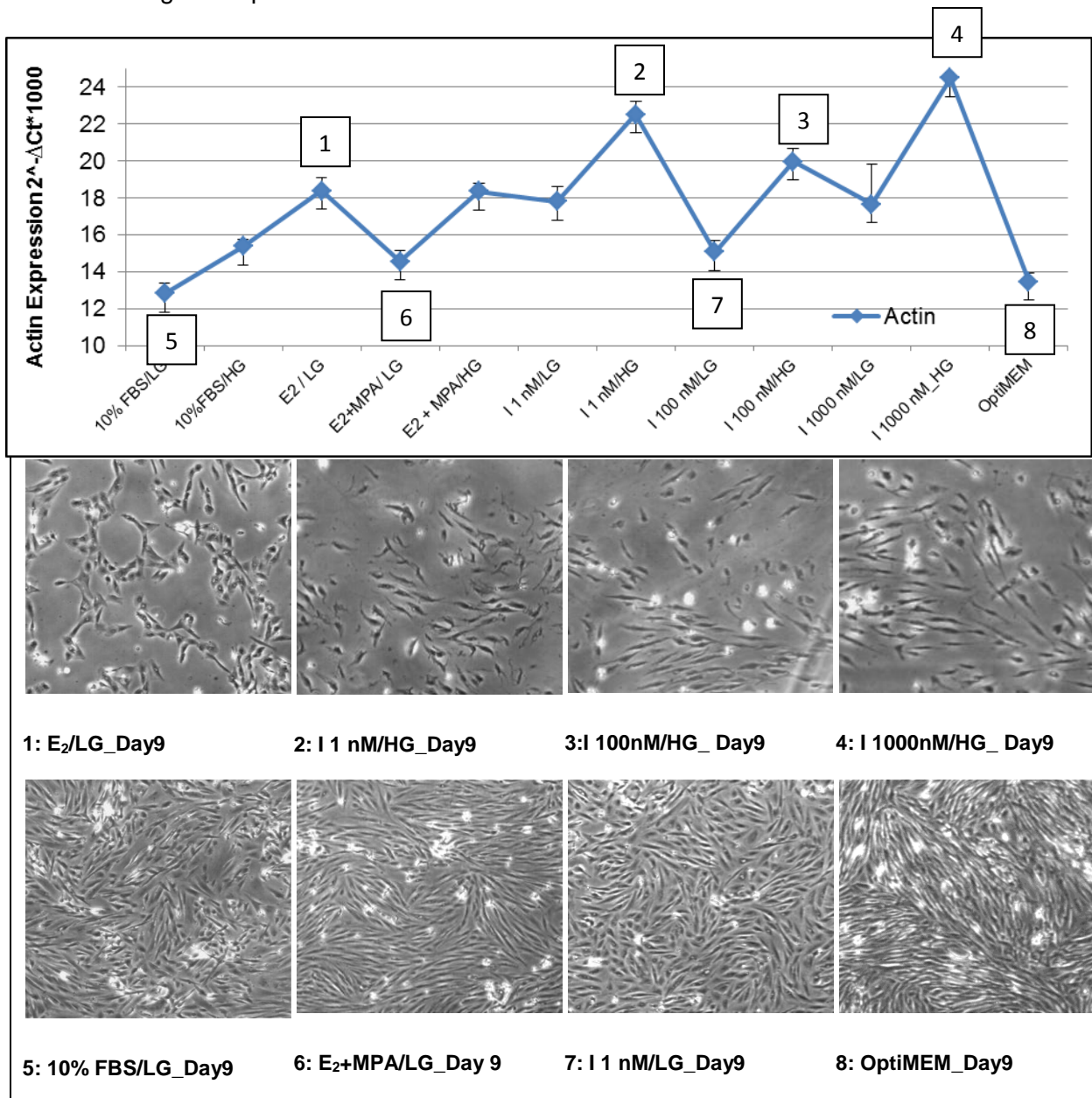


Figure 30: Actin expression plus corresponding microscopic bright field cell morphology pictures of different treatment groups after eight days of decidualization protocol. Data in the graph show mean values +/- SEM. Numbers in the graph correspond to the numbers below the microscopic images.

5. Discussion and conclusion

This bachelor project examined whether glucose and insulin affect the process of cell growth and differentiation in a model of decidualization. Cell counts obtained across the growth curve project suggest that HESCs tend to grow better in low glucose medium than in high glucose medium. These findings may be explained by the actual doses of glucose contained in the different media: While low glucose medium mimics the physiological blood glucose level, glucose concentrations are in a pathophysiological range in the high glucose medium. Contrary to what was expected, the addition of insulin into both media did not change the cell growth outcome.

However, these findings may have been compromised by two factors: For one, a growth interval of five days might be too short to lead to final conclusions of cell growth behavior. It was not determinable how cells would continue their growth after day five (Figure 26). Secondly, there was a possible impairment of cell growth through the occurrence of cell death during the protocol, which probably had some influence on cell numbers counted and could have led to false results (Figure

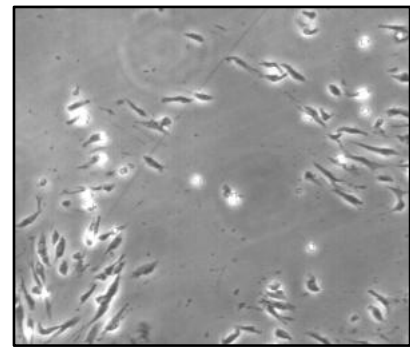


Figure 31: Cell death

31). For more significant results, it is therefore recommendable to repeat growth curves with a greater number of cell samples, a longer observation time and - most importantly - healthy growing cells.

As occurring cell death had averted the use of ELISA techniques, qRT-PCR was used to determine the prolactin expression of HESCs involved in decidualization projects. Data obtained from those qRT-PCRs were characterized by a great inconsistency. They did however show a pattern when it came to their differentiation rate in high glucose vs. low glucose media. While low glucose seemed to boost cell proliferation, high glucose was shown to promote cell differentiation.

A second finding was made by analyzing final prolactin values calculated by subtracting actin expression values from prolactin expression values. It became clear that the housekeeping gene actin had shown more irregular expression curves than the actual targeted gene prolactin. In the following, two hypotheses for such an irregularity were found.

First, there might be a link between cells with low actin expression and their growth in high glucose. Cells cultured in high glucose medium showed much less actin concentration as cells cultured in low glucose medium which might indicate more changes within the gene expression patterns of high glucose groups.

Second, cells with very low actin expression could be associated with ongoing cell death by relying on pictures taken during the decidualization protocols. This correlation suggests that dying cells could experience changes in actin expression rates as their cytoskeleton is involved in mechanisms related to apoptosis.

In summary, the here described project did indeed lead to interesting conclusions. The hypothesis which indicated that HESCs are sensitive towards different glucose concentrations and insulin doses could be verified. Both of those substances induced significant differences when it comes to differentiation and proliferation capacities of HESCs.

Nevertheless, challenges such as infection or cell death had to be overcome during the cell culture processes. They made it difficult to rely on results obtained. On this ground, it would be most recommended to repeat both growth curve and decidualization project before come to final conclusions about possible influences of insulin and/or glucose concentrations on differentiation or proliferation rates. Also, the use of another housekeeping gene besides actin should be performed in order to determine the actual differentiation process of treated cells with a stable internal control.

Despite the limitations of these experiments, this project may have set ground for further investigations on a possible link between HESCs and their insulin and glucose concentration sensitivity. If the here obtained results were shown to be reproducible on further testing, then further research could lead to better understanding of how obesity and diabetes affect fertility.

6. References

Alberts B, Johnson A, Lewis J, Raff M, Roberts K, Walter P. 2008. Molecular biology of the cell. 5th edition. Garland Science, Taylor & Francis Group. p. 360-285.

Brosens JJ, Hayashi N, White JO. 1999. Progesterone receptor regulates decidual prolactin expression in differentiating human endometrial stromal cells. *Endocrinology*. 140(10):4809-20.

Brothers KJ, Wu S, DiVall SA, Messner MR, Kahn Cr, Miller RS, Radovick S et al. 2010. Rescue of obesity-induced infertility in female mice due to a pituitary-specific knockout of the insulin receptor. *Cell Metabolism* 295-305.

Burtis CA, Aswood ER, Bruns DE. 2012. Tietz Textbook of clinical chemistry and molecular diagnostics. 5th edition. Elsevier Saunders. p. 391- 392.

ELISA technique.

<http://www.elisa-antibody.com/> <02.06.2013>

Fritz MA, Speroff L, 2011. Clinical gynecologic endocrinology and infertility. 8th Edition. Lippincott Williams & Wilkins. p. 124 - 131.

Ganef C, Chatel G, Munaut C, Frankenne F, Foidart JM, Winkler R. 2008. The IGF system in in-vitro human decidualization. *Molecular Human Reproduction*. 15(1): 27–38

Gellersen B, Brosens IA, Brosens JJ. 2007. Decidualization of the human endometrium: mechanisms, functions, and clinical perspectives. *Seminars in Reproductive Medicine*. 25(6):445-53.

Guerin LR, Prins JR, Robertson SA. 2009. Regulatory T-cells and immune tolerance in pregnancy: a new target for infertility treatment? *Human reproductive update*. 15: 517-535.

Gurpide E, Abanelli S, Tang B. 1992. In vitro decidualization of human endometrial cells. *Journal of biochemistry and molecular biology*. 4(3/4): 337-344>

High glucose DMEM, www.invitrogen.com

http://www.invitrogen.com/site/us/en/home/support/Product-Technical-Resources/media_formulation.8.html<17.05.2013>

Hoffmann BL, Schorge JO, Schaffer JI, Halvorson LM, Bradshaw KD, Cunningham FG, 2012. Williams Gynecology. 2nd edition. The McGraw Hill. p. 432-434.

Holt R, Cockram CS, Flyvbjerg A, Golstein BJ et al. 2010. Textbook of diabetes. 4th edition. Blackwell Publishing Ltd. p. 87-99 / p. 104-119.

<http://www.elisa-antibody.com/> Sandwich Elisa, highly sensitive. <10.05.2013>

Jameson JL, De Groot LJ, De Kretser D, Grossman A, Marshall JC, Melmed S, Potts JT JR et al. 2010. Endocrinology adult and pediatric. 6th edition. Saunders Elsevier. p. 603-614.

Kawamoto S JD, McClure D, Sato G. 1983. Development of a serum-free medium for growth of NS-1 mouse myeloma cells and its application to the isolation of NS-1 hybridomas. *Analytical Biochemistry*. 130. 445-453.

Koopman LA, Kopcow HD, Rybalov B, et al. 2003. Human decidual natural killer cells are a unique NK cell subset with immunomodulatory potential. *Journal of Experimental Medicine*. 198:1201– 1212.

Lenz GM, Lobo RA, Gershenson DM, Katz VL, 2012. *Comprehensive Gynecology: Expert consult online and print*. Elsevier Mosby. http://books.google.com/books?id=X5KT_w6Nye8C&printsec=frontcover&hl=de&source=gbs_ge_summary_r&cad=0#v=twopage&q&f=false <25.02.2013>

Lin J, Redies C. 2012. Histological evidence: housekeeping genes beta-actin and GAPDH are of limited value for normalization of gene expression. *Development genes and evolution* 222(6):369-76

Lodish H, Berk A, Kaiser, CA, Krieger M, Bretscher A, Ploegh H, Amon A. 2013 *Molecular cell biology*. 7th edition. W.H. Freeman and Company. p. 190-200.

Longo D, Fauci A, Kasper D, Hauser S, Jameson J, Loscalzo J. 2012. *Harrison's manual of medicine*. 18th edition. McGraw Hill. P. 1137-1144.

Low glucose DMEM, www.invitrogen.com
http://www.invitrogen.com/site/us/en/home/support/Product-Technical-Resources/media_formulation.48.html <17.05.2013>

McPherson RA, Pincus MR, Abraham NZ, Bluth MH, Bock JL, Hutchison RE, Massey HD, Miller JL et al. 2011 *Henry' clinical diagnosis and management by laboratory methods*. 22nd edition. Elsevier Saunders. p. 1270-1280

Nayak NR, Giudice LC. 2003. Comparative biology of the IGF system in endometrium, decidua, and placenta, and clinical implications for foetal growth and implantation disorders. *Placenta* 24:281–296

RNeasy® Mini Handbook. 2010. 4th edition.
<http://www.qiagen.com/Products/Catalog/Sample-Technologies/RNA-Sample-Technologies/Total-RNA/RNeasy-Mini-Kit#productdetails>. <13.03.2013>

Salker M, Teklenburg G, Molokhia M, Lavery S, Trew G, et al. 2010. Natural selection of human embryos: Impaired decidualization of endometrium disables embryo-maternal interactions and causes recurrent pregnancy loss. *PLoS ONE* 5(4): e10287.

Thannickal VJ, Fanburg BL. 2000. Reactive oxygen species in cell signaling. *American Journal of Physiology. Lung and cell molecular physiology*. 279: L1005–L1028.

7. Table of figures

Figure 1: Insulin

<http://www.life-enhancement.com/images/insulin1.gif> <09.05.2013>

Figure 2: Insulin synthesis

http://www.betacell.org/content/articlepanelview/article_id/1/panel_id/1. <08.04.2013>

Figure 3: Insulin action

<http://www.idf.org/sites/default/files/Insulin-production-and-action.jpg>. <15.04.2013>

Figure 4: Insulin and glucose metabolism within the cell

http://upload.wikimedia.org/wikipedia/commons/8/8c/Insulin_glucose_metabolism.jpg. <15.04.2013>

Figure 5: Type 1 and type 2 DM

<http://foodstoriesblog.com/what-is-diabetes/> <01.03.2013>

Figure 6: Functional anatomy of the human endometrium

http://o.quizlet.com/i/owgamtPGjq5m9AzltW704Q_m.jpg. <25.02.2013>

Figure 7: Endometrial tissue during secretory phase

<https://courses.stu.qmul.ac.uk/smd/kb/microanatomy/humandev/images/t/hd24t.jpg>. <16.02.2013>

Figure 8: Endometrial transformation during the menstrual cycle

<http://www.pfcla.com/wp-content/uploads/2012/05/menstrual-cycle-hormone-levels1.png> <01.03.2013>

Figure 9: Changes of cell morphology during decidualization

<https://www.thieme-connect.com/ejournals/html/10.1055/s-2007-991042-> <16.05.2013>

Figure 10: Implantation

http://php.med.unsw.edu.au/embryology/images/thumb/2/2b/Implantation_LIF.jpg/700px-Implantation_LIF.jpg <18.04.2013>

Figure 11: Trophoblast invasion and signaling

<http://ars.els-cdn.com/content/image/1-s2.0-S0165037810004055-gr1.jpg> <20.04.2013>

Figure 12: Estimated rates of fetal mortality by weeks of gestation

<http://www.aafp.org/afp/2007/1101/afp20071101p1341-f1.gif> <21.04.2013>

Figure 13: Impact of cAMP+MPA on decidualization by Brosens et al.
<http://endo.endojournals.org/content/140/10/4809.long> <21.04.2013>

Figure 14: Pregnancy rates per stimulation by age and BMI
<http://www.advancedfertility.com/weight.htm> <25.04.2013>

Figure 15: Plate design. Self-made figure.

Figure 16: Cutting biopsy material with razor blade. Self-taken picture.

Figure 17: Covering well with trypsin. Self-taken picture.

Figure 18: Haemocytometer
<http://www.78steps.com/enzyme-immobilization/encapsulation-of-cells-in-alginate-gels.html> <10.05.2013>

Figure 19: Antibody-antigen-antibody complex
http://www.activemotif.com/images/products/nr_sandwich.jpg <10.05.2013>

Figure 20: Sandwich ELISA
http://www.epitomics.com/images/products/sandwich_dual.jpg. <10.05.2013>

Figure 21: Schema of Transcription
<http://www.vcbio.science.ru.nl/en/virtuallessons/cellcycle/trans/> <12.93.2013>

Figure 22: Qiagen's protocol for RNA extraction
http://abe.leeward.hawaii.edu/Protocols/RNeasy%20Principle_files/image002.jpg
<13.03.2013>

Figure 23: Synthesis of cDNA
<http://9e.devbio.com/images/ch04/0405fig2.jpg> <13.03.2013>

Figure 24: SYBR green action during qRT-PCR
http://www.nfstc.org/pdi/Subject03/images/pdi_s03_m05_07_a.gif. <10.05.2013>

Figure 25: Growth curve: comparison of low and high glucose. Cumulative data of four separate experiments in primary endometrial stromal cells, with each experiment completed in duplicate. Data show mean value +/- standard error of mean (SEM). Self-made figure.

Figure 26: Growth curve: comparison of cell growth in media containing low glucose (LG), low glucose plus 100 nM insulin (LG + I 100), high glucose (HG) and high glucose plus 100 nM insulin (HG + I 100), in primary endometrial cells. Data are representative of two separate experiments, each in duplicate. Data show mean value +/- standard error of mean (SEM). Self-made figure.

Figure 27: Fold change in prolactin expression in different treatment groups after 8 days of decidualization treatment. Data show mean value +/- standard error of mean (SEM). Self-made figure.

Figure 28: Actin expression vs. prolactin expression. Data show mean value +/- standard error of mean (SEM). Self-made figure.

Figure 29: Actin expression in low glucose vs. high. Data show mean value +/- standard error of mean (SEM). Self-made figure.

Figure 30: Actin expression plus corresponding cell morphology picture of different treatment groups after eight days of decidualization protocol. Data show mean value +/- standard error of mean (SEM). Self-made figure.

Figure 31: Cell death. Self-taken picture.

8. Appendix

Growth curve of cells # 151, #153, #154 and #151b in low glucose and high

glucose. Five day protocol

	151a LG1	151a LG2	151a LG3	153 LG1	153 LG2	153 LG3	154 LG 1	154 LG 2	151 bLG 1	151 bLG 2	MEA N	SEM
0 h	8	5,5	6	8	10	4	3,25	2	2,25	4	5,30	0,85
day 1	16,25	19	16,5	12	12,5	7,25	4	3	4,75	6,5	10,18	1,84
day 3	31,5	36,25	38,25	10,75	10	10	5,75	5,25	13	13,75	17,45	4,03
day 5	35,75	30	31,75	18	12	11,75	16,25	9,25	20	21,75	20,65	2,89

	151a HG1	151a HG2	151a HG3	153 HG1	153 HG2	153 HG3	154 HG1	154 HG2	151 bHG1	151b HG2	MEA N	SEM	P- VALUE
0 h	6,5	6	7,25	5,5	3,25	3,5	2	2	3,25	3,5	4,31	0,60	0,34
day 1	8,5	15	16	8	7,75	7,75	4	6,25	4,5	3,5	8,16	1,35	0,38
day 3	26	18,25	24,75	8,5	10	7,75	11,75	14	14,25	9,75	14,55	2,06	0,53
day 5	27,25	19,75	26,25	9	13	9,75	9,75	9,25	8,5	16	14,86	2,29	0,13

Growth curve of cells #154 and #151b in low glucose, high glucose, low glucose + insulin 100 nM and high glucose + 100 nM. 5 day protocol

DAY 0	154 LG 1		151b LG 1		154 HG 1		151b HG 1		154 LG 100		151b LG 100		154 HG 100		151b HG 100	
	square 1	square 2	square 3	square 4	square 1	square 2	square 3	square 4	square 1	square 2	square 3	square 4	square 1	square 2	square 3	square 4
mean	6	2	2	3	2	2	2	4	2	2	3	4	2	2	1	4
SEM	2,25	2	1	4	2	2	0	4	1	1	1	5	2	1,75	3	1,75
DAY 1	154 LG 2		151b LG 2		154 HG 2		151b HG 2		154 LG 100		151b LG 100		154 HG 100		151b HG 100	
square 1	3	4	6	7	3	7	4	5	5	5	9	5	5	6	3	3
square 2	7	2	6	8	5	6	5	2	4	3	5	7	8	6	2	5
square 3	3	3	4	4	5	7	6	4	5	2	4	4	7	7	3	3
square 4	3	3	3	7	3	5	3	3	4	3	3	5	4	7	9	5
mean	4	3	4,75	6,5	4	6,25	4,5	3,5	4,5	3,25	7,5	5	6,75	7	4,5	4
SEM	5,75	5,25	13	13,75	11,75	14	14,25	9,75	7,25	6,5	11,25	16,75	11	24,25	9	8,75
DAY 3	154 LG 1		151b LG 1		154 HG 1		151b HG 1		154 LG 100		151b LG 100		154 HG 100		151b HG 100	
square 1	5	5	11	6	9	14	11	11	11	6	12	17	8	28	7	9
square 2	9	7	15	24	15	12	15	15	7	9	12	19	16	30	15	10
square 3	4	5	12	9	9	18	18	7	6	6	10	15	16	23	6	10
square 4	5	4	14	16	14	12	13	6	5	5	11	16	4	16	8	6
mean	5,75	5,25	13	13,75	11,75	14	14,25	9,75	7,25	6,5	11,25	16,75	11	24,25	9	8,75
SEM	15	7	22	32	9	7	9	20	9	6	23	44	4	10	10	25
DAY 5	154 LG 1		151b LG 1		154 HG 1		151b HG 1		154 LG 100		151b LG 100		154 HG 100		151b HG 100	
square 1	19	13	21	13	11	16	9	26	6	5	20	25	4	5	16	18
square 2	15	8	19	18	10	8	8	12	6	10	20	22	10	7	8	29
square 3	16	9	18	24	9	6	8	6	5	5	17	40	6	4	8	21
mean	16,25	9,25	20	21,75	9,75	9,25	8,5	16	6,5	6,5	20	32,75	6	6,5	10,5	23,25

MEAN	Day 0	SEM	Day 0	P-Values	Day 0	MEAN	Day 3	Sem	Day 3	P-Value	Day 3
LG	3	LG	0,46	LG/HG	0,55	LG	9	LG	2,28	LG/HG	0,12
HG	3	HG	0,40	LG/LG 100	0,82	HG	12	HG	1,06	LG/LG 100	0,58
LG + 100	3	LG + 100	0,84	HG / HG 100	0,23	LG + 100	8	LG + 100	2,35	HG / HG 100	0,71
HG + 100	2	HG + 100	0,30	LG + HG / LG	0,34	HG + 100	13	HG + 100	3,70	LG + HG / LG	0,53
MEAN	Day 1	SEM	Day 1	P-Value	Day 1	MEAN	Day 5	SEM	Day 5	P-Value	Day 5
LG	5	LG	0,74	LG/HG	0,32	LG	17	LG	2,77	LG/HG	0,01
HG	5	HG	0,60	LG/LG 100	0,51	HG	11	HG	1,73	LG/LG 100	0,96
LG + 100	5	LG + 100	0,89	HG / HG 100	0,12	LG + 100	11	LG + 100	6,30	HG / HG 100	0,78
HG + 100	6	HG + 100	0,77	LG + HG / LG	0,12	HG + 100	12	HG + 100	4,02	LG + HG / LG	0,94

PCR results 8 day decidualization protocols for primary human endometrial stromal cells # 151a and 151b done at separate times

Dates of RNA Extraction: # 151a 5/3/13		# 151b 5/7/13											
Sample	#151 10% FBS/LG	#151 10% FBS/HG	# 151E2/LG	# 151E2+MPA/LG	#151E2+MPA/HG	# 1511nMLG	# 1511nMHG	#151100nMLG	#151100nMHG	#1511000nMLG	#1511000nMHG	#1511000nLHG	#1510nMEM
1	11,85	15,59	17,78	14,57	15,94	17,44	23,47	15,75	21,38	17,96	23,32	13,12	
2	12,21	15,54	17,93	15,12	16,04	17,13	23,17	15,00	21,17	17,66	23,50	13,00	
mean	12,14	15,41	17,93	14,69	15,89	17,13	23,17	15,00	21,17	17,66	23,50	13,05	
PROLACTIN #151a													
1	27,42	29,14	25,99	27,59	27,74	30,89	27,27	30,37	27,99	29,91	27,29	22,89	
2	27,08	28,92	25,89	27,26	27,13	29,86	26,34	28,68	28,30	28,55	26,86	23,22	
3	27,88	29,54	27,49	27,69	27,69	27,69	27,69	29,53	28,15	29,23	27,08	23,07	
mean	27,46	29,2	25,94	27,46	27,52	30,38	27,08	29,53	28,15	29,23	27,08	23,06	
ΔCt	15,32	13,79	8,02	12,76	11,63	13,25	3,91	13,53	6,98	11,57	3,58	10,01	
SEM													
2 ^{-ΔΔCt} *1000	0,02	0,07	3,87	0,14	0,32	0,10	66,52	0,08	7,32	0,33	83,91	0,97	
Fold change	2,87	54,88	5,90	12,88	4,19	2714,87	3,45	323,29	13,42	3424,47	39,58		
ACTIN #151b													
1	11,99	16,50	18,77	14,60	17,62	17,76	23,31	14,14	19,85	18,02	21,96	13,47	
2	12,20	15,99	18,93	14,69	18,34	18,00	23,34	14,57	20,00	17,64	22,03	13,76	
mean	12,10	16,25	18,85	14,65	17,98	17,88	23,33	14,36	19,93	17,83	22,00	13,62	
PROLACTIN #151b													
1	27,43	28,78	27,90	28,00	28,82	26,98	28,19	28,15	28,92	27,68	28,42	24,66	
2	27,38	29,87	27,03	28,11	27,81	27,03	28,68	27,93	28,59	28,61	28,61	24,74	
mean	27,41	29,33	27,47	28,56	28,32	27,01	28,44	28,54	28,76	27,68	28,52	24,70	
ΔCt	15,21	13,34	8,54	13,87	9,98	9,01	5,10	13,97	8,76	10,04	6,49	10,94	
SEM													
2 ^{-ΔΔCt} *1000	0,03	0,10	2,70	0,07	0,99	1,95	29,26	0,06	2,31	0,95	11,16	0,51	
Fold change	3,66	101,83	10,83	2,53	37,53	73,52	1105,13	2,35	87,43	35,88	421,68	19,23	



PCR results 8 day decidualization protocols for primary human endometrial stromal cells # 153a and 153b done at separate times

Dates of RNA Extraction: # 153 a 5/3/13 # 153b 5/12/13													
Sample	#153 10% FBS/LG	#153 10% FBS/HG	#153 E2/LG	#153 E2+MPA/LG	#153 E2+MPA/HG	#153 11nM/LG	#153 11nM/HG	#153 100 nM/LG	#153 100 nM/HG	#153 1000 nM/LG	#153 1000 nM/HG	#153 OptiMEM	
ACTIN #153a													
1	13,86	14,13	17,70	13,53	18,68	18,64	22,07	14,60	18,71	18,88	20,36	13,16	
2	13,73	14,71	17,73	13,85	18,71	18,42	22,53	14,96	18,75	18,34	20,35	12,93	
3	13,73											13,53	
mean	13,77	14,42	17,72	13,69	18,70	18,53	22,30	14,78	18,73	18,61	20,36	13,21	
PROLACTIN #153a													
1	27,36	28,63	27,51	25,30	27,66	28,23	28,22	27,75	27,16	27,93	26,87	24,24	
2	28,55	27,39	26,35	26,43	27,75	26,34	27,76	27,69	27,78	26,91	26,72	24,80	
3	29,03											25,19	
mean	28,31	28,01	26,93	26,17	27,71	27,29	27,99	27,72	27,47	27,42	26,80	24,74	
ΔCt	14,54	13,59	9,22	12,48	9,01	8,76	5,69	12,94	8,74	8,81	6,44	11,54	
SEM													
2 ^{-ΔCt} *1000	0,04	0,08	1,68	0,18	1,94	2,31	19,37	0,13	2,34	2,23	11,52	0,34	
Fold change	1,93	4,09	4,18	46,21	55,14	461,44	55,72	3,03	53,08	274,37	8,02		
ACTIN #153b													
1	13,31	20,59	18,90	15,00	20,81	17,70	21,29	14,30	20,68	16,27	29,68	13,86	
2	13,29	20,89	19,20	15,23	20,82	17,70	21,21	15,38	20,89	17,08	29,54	13,98	
mean	13,30	20,74	19,05	15,12	20,82	17,70	21,25	15,14	20,79	16,68	29,61	13,92	
PROLACTIN #153b													
1	30,46	31,19	29,39	28,64	29,51	28,83	30,25	30,76	30,17	19,76	30,19	29,09	
2	28,89	29,15	29,31	28,75	29,68	30,05	30,64	30,69	22,98	19,26	30,79	23,16	
mean	29,68	29,35	29,35	28,70	29,60	29,44	30,45	30,73	19,51	19,51	30,49	23,16	
ΔCt	16,38	13,58	10,30	13,58	8,78	11,74	9,20	15,59	2,84	0,88	9,24		
SEM													
2 ^{-ΔCt} *1000	0,01	0,79	0,08	2,27	0,29	1,71	0,02	140,15	543,37	1,65			
Fold change	67,42	193,34	24,85	145,01	11910,94	46180,62	140,56						